Elsevier Editorial System(tm) for Talanta
Manuscript Draft

Manuscript Number: TAL-D-18-00532R1

Title: AN INTEGRATED STRATEGY TO CORRELATE AGGREGATION STATE, STRUCTURE AND TOXICITY OF Aß 1-42 OLIGOMERS.

Article Type: Research Paper

Keywords: Alzheimer's disease; Capillary electrophoresis; Aß 1-42; Aß oligomers; Sample preparation; Fourier transform infrared spectroscopy.

Corresponding Author: Professor Ersilia De Lorenzi,

Corresponding Author's Institution: University of Pavia

First Author: Federica Bisceglia, MSc

Order of Authors: Federica Bisceglia, MSc; Antonino Natalello, PhD; Melania M Serafini, MSc; Raffaella Colombo, PhD; Laura Verga, PhD; Cristina Lanni, PhD; Ersilia De Lorenzi

Abstract: Despite great efforts, it is not known which oligomeric population of amyloid beta (Aß) peptides is the main neurotoxic mediator in Alzheimer's disease. In vitro and in vivo experiments are challenging, mainly because of the high aggregation tendency of Aß (in particular of Aß 1-42 peptide), as well as because of the dynamic and non covalent nature of the prefibrillar aggregates. As a step forward in these studies, an analytical platform is here proposed for the identification and characterization of Aß 1-42 oligomeric populations resulting from three different sample preparation protocols. To preserve the transient nature of aggregates, capillary electrophoresis is employed for monitoring the oligomerization process in solution until fibril precipitation, which is probed by transmission electron microscopy. Based on characterization studies by ultrafiltration and SDS-PAGE/Western Blot, we find that low molecular weight oligomers build up over time and form bigger aggregates (> dodecamers) and that the kinetics strongly depends on sample preparations. The use of phosphate buffer results to be more aggregating, since trimers are the smallest species found in solution, whereas monomers and dimers are obtained by solubilizing Aß 1-42 in a basic mixture. For the first time, attenuated total reflection-Fourier transform infrared spectroscopy is used to assign secondary structure to the separated oligomers. Random coil and/or α-helix are most abundant in smaller species, whereas ß-sheet is the predominant conformation in bigger aggregates, which in turn are demonstrated to be responsible for Aß 1-42 toxicity.

Talanta

Editor-in-Chief for Europe

Prof Jean-Michel Kauffmann

Dear Prof Kauffmann,

please find here our manuscript entitled

AN INTEGRATED STRATEGY TO CORRELATE AGGREGATION STATE, STRUCTURE AND TOXICITY OF Aß 1-42 OLIGOMERS.

by myself and Federica Bisceglia, Antonino Natalello, Melania Maria Serafini , Raffaella Colombo, Laura Verga and Cristina Lanni

The paper is unpublished and has not been submitted for publication elsewhere.

Despite great efforts, it is not known which oligomeric population of amyloid beta (Aß) peptides is the main neurotoxic mediator in Alzheimer's disease and in particular the relationship between size, structure and toxicity of Aß42 oligomers remains unclear.

As a step forward in these studies (including our pioneering work published in 2004), a standardised analytical platform is here proposed for the identification and characterization of Aß 1-42 oligomeric populations resulting from three different sample preparation protocols.
The methods and techniques employed include capillary electrophoresis, transmission electron microscopy, SDS-PAGE/Western Blot, ultrafiltration, attenuated total reflection-Fourier transform infrared spectroscopy and cell toxicity studies.
Particular attention has been paid to: the reproducibility of sample preparation protocols, the sample solubility and supplier-to supplier variability, the reproducibility of analytical data, the dynamic equilibria in solution, the assignment of size, secondary structure and toxicity to the capillary electrophoresis-separated oligomers.
A substantial improvement and advantage over existing methods is here reported and the applicability of the analytical methods is of interest to a wide scientific community.

We hope that the manuscript is suitable for publication in Talanta.

On behalf of myself and my co-authors I look forward to hearing from you

Sincerely

Prof. Ersilia De Lorenzi

Corresponding author
Email: ersidelo@unipv.it
Department of Drug Sciences
Viale Taramelli 12
University of Pavia

Questions have been arbitrarily numbered for the sake of clarity.

Pages and lines refer to the Word new version of the manuscript

Reviewer #1:

This is interesting work on the important topic of characterising amyloid-beta (Ab) oligomers of different sizes. These were obtained from different suppliers, prepared by different protocols and studied with a number of techniques. It is found that the oligomer distribution depends on the preparation protocol and that oligomers of different sizes have different FTIR spectra. My comments are as follows:

1) Some abbreviations are not explained: EOF, SD, DAD.

The abbreviations have been added in text: EOF P1 L33 and P6 L171, DAD P6 L 158, SD P8 L243.

2) P5 L53, the statement that the samples were not centrifuged seems to be in contrast with the use of ultrafiltration.

We intended to avoid mechanical stress *at the beginning of the aggregation process*. This has been added in text (P5 L151,152).

Ultrafiltration is instead performed at different elapsed times from solubilization, when oligomers are formed. The comparison of retained/filtrated peaks with those of non filtrated peptide confirms that the process does not induce mechanical stress.

3) P10 L5ff and Fig. 1, are the traces shown in Fig. 1 averages from 5 experiments, or are they from individual experiments?

Electropherograms reported in figures are representative of one out of five independent experiments (n=5). To make this clearer it was added both in text (P9 L275) and in captions (Figure 1,2,3).

The unit of effective mobility should be given in Fig. 1.

As suggested by the reviewer, the unit of mobility ($cm^2V^{-1}s^{-1}$) has been added both in text (P6 L173-174) and in tables included in Figure 1 and 3.

Data for only 7 time points are shown although 10 time points were collected. Why?

A selection of traces was made to simplify the figure.

4) P11 L5 and Fig. S3b, there is no spectrum in the inset.

As now indicated, the inset of Figure S3b) reports the UV spectrum taken at the apex of peak C (time: 10.187 min).

5) P12 L1 and Fig. S4, why do all species disappear with time?

As already mentioned in text (P11 L322-324) the "disappearance of peaks" or the absence of peaks in the electropherograms is reasonably ascribed to insoluble

material that precipitates at the bottom of the vial and thus is not injected (P10 L 295-297). As already discussed in text, the simultaneous precipitation of formed species in this particular case would be consistent with the observation of lack of equilibrium between formed species (as opposed to the sequential precipitation when equilibrium is observed).

6) P12 L36, what is the evidence for fibrils in the t0 sample?
We think that the legend to Figures is already clear. Nevertheless, to make clearer that the TEM image refers to fibrils at t0, the sentence in text (P12 L372-373) was rephrased as follows:
"In Figure 3a) it is clear that at t0 the sample already includes at least three main electrophoretic peaks as well as amyloid fibrils, which are observed by TEM. "

7) P12 L43, the mobilities of peak 1 and peak A are very similar, so I would not state that they are different.
We agree with the reviewer on this comment confined to peak A and 1 mobilities. The sentence has been rephrased as follows (P 12 L 377-380):
"In Figure 3a), mobilities are calculated as average of 5 independent experiments using three peptide batches from the same supplier. Effective mobilities are statistically different from those reported in Figure 1a), except for those of the fastest migrating peak, where values fall within the experimental errors, equal to two times the standard deviation [45]. However, they are labelled as peak 1, 2 and 3."
The new reference has been added as ref [45].

8) P12 L51 and throughout text, presence or absence of a dynamic equilibrium is mentioned at several places without giving evidence for the statement. Throughout the experiment, the sample is not in equilibrium because aggregation is ongoing.
We confine the term dynamic equilibrium (as we did in refs [21, 26-28]) to the detected population of soluble oligomers which is depleted to build up larger oligomers, as evident from graphs in the Figures.

9) P13 L1, there seems to be an apparent contradiction between the statement that Ab42 oligomers are soluble for one month and the statement that the t0 sample contained fibrils.
We would like to point out that there is no contradiction, only soluble material is injected in CE and this does not exclude the presence of fibrils at the bottom of the anodic vial, where injection takes place. This was already clearly reported at P10 L293-298: "Transmission electron microscopy (TEM) image taken at t0 in Figure 1a), representative of three independent experiments, reveals that also fibrils are present

in this sample: as the solution is neither stirred nor centrifuged before analysis, it is likely that they are sedimented at the bottom of the anodic vial and thus they are not injected into the capillary, as confirmed by the absence of spikes in the electropherogram. Since oligomers and fibrils are at equilibrium in the brain [9] this protocol better mimics in vivo conditions, as compared to protocols that force the apparent formation of monomers [22].”

10) P13 L24, explain why precipitation is concluded from the flat CE trace in Fig. S5 of the Bachem sample.

For the explanation required TEM image of fibrils at t30 min is added to Figure S5 and the sentence at P13 L402-404 has been rephrased as follows:

“Conversely, when Aß42 provided by Bachem is solubilized by following protocol #1, precipitation occurs after 30 minutes from t0, when soluble species are not detected, the sample is visibly cloudy and TEM analysis shows fibrils (Figure S5).”

11) P14 L14-29, peak C is retained by 100 kDa filtration, so the corresponding aggregates should be larger than 100 kDa in contrast to what is said in the text.

To clarify this statement, the comment to Fig 4a (100kDa UF) has been edited (P14 L 428-434).

Within the range of the broad peak B there are two sharp peaks in the CE trace of the retained solution after 100 kDa filtration. What are these?

Most peptide is filtrated, therefore the retained portion is negligible (Fig.4a). As generally declared in text when introducing these membranes (P14 L419-422) “the amount found in the retained solution can partly be constituted by aggregated peptide adsorbed on the filter and not necessarily retained in virtue of its size”. This can be well the case when the retained portion is negligible.

Peak 3 is neither present in the retained nor filtrated volume when the 100 kDa membrane is used. Please comment.

Once again, (bearing in mind P14 L419-422) in this case the low recovery of filtrated peptide migrating under peak 3 (Figure 4a) is more reliable that the low recovery of retained peptide under peak B-C (Figure 4a). It is assumed that part of the peptide is entrapped in the filter. This comment has been added to the text (P14 L434-436).

The last sentence in this paragraph has a logical problem, first it is said that the same conclusions were obtained with ultrafiltration as before, then that some observations can only be done with CE.

We agree that here the sentence is not clear and for this reason it was misunderstood by the reviewer. What it was intended here is: 1. that the presence of monomers and dimers, as demonstrated in [20], is confirmed; 2. that a long-time monitoring of small oligomers has been described only in this paper, by using CE.

The sentence "By simple ultrafiltration experiments the same conclusions as derived by [20] are obtained; notably, that small oligomers are detected and accurately monitored in solution for weeks is appreciated by CE only."
has been rephrased as follows (P14 L440-442):
"By simple ultrafiltration experiments the presence of monomers and dimers in solution, as demonstrated in [20], is confirmed. It is valuable that in this work the presence of soluble Aß oligomers is monitored for much longer time.

12) P15 L25, good to have solution FTIR spectra also!
We are pleased that the reviewer appreciates.

13) P15 L33-39, time is missing for some of the beta sheet contents.
Time has been added both in text (P14 L 449, P15 L 465-466), in Figures 5, S6, S7 and to relative captions.

14) P15 L44, the last half sentence is unclear and probably unnecessary.
We agree with the reviewer. The last half sentence has been deleted (P16 L485-486).

15) Fig. 1 lacks annotation of the horizontal axis.
We apologise for this oversight. Annotation has been added to Figures 1 and 3.

Reviewer #2:

In this paper, the authors described the development of multiple approaches to study Amyloid beta 1-42 aggregation, structure and toxicity.

The overall strategy and the analytical protocol are well described; the observations are critically discussed regarding the existing literature. This research topic is very controversial because it is very difficult to make the difference between information coming from the original sample and the artifact caused by the sample preparation and/or the analytical method. This is why an integrated approach, as described here, is a good practice, even if it is not yet perfect.

I have some questions and concerns about the work:

1) how the authors could explain the big differences between the oligomeric forms observed in the CE conditions of Figure 1 (Peak A, B and C) versus Figure 3 (Peak 1, 2 and 3)?

As stated at P3 L81-82 it is known that "Each specific solubilization protocol (different solvents, peptide concentrations, incubation time and temperature) leads to different oligomeric species [11, 12]". In our work different sample preparation protocols are selected to finely tune aggregation and lead to different oligomeric populations.

2) some peak tailing (Figures 1, 2 and 3) seems to indicate that interactions with the capillary wall occur, could those unwanted interactions, as well as the application of a strong voltage during separation, influence the oligomerization/aggregation kinetic?

In particular in Figures 1 and 3 (that contain data used for characterization) we do not see a strong peak tailing. Further, the excellent RSDs obtained, the absence of spikes and the stable current rule out unwanted interactions with the capillary wall (P10 L 280-282). This comment has been added in text (P10 L283).

For this reason we did not use a coated capillary.

As far as the strong voltage, we already addressed this issue in [21]. In this work the same current as in our previous works [21, 26] was kept, thus we draw the same conclusion as in [21], where we demonstrate that the electric field does not influence the strength of the noncovalent intermolecular interactions that sustain the peptide oligomerization.

This observation has been now added in text at P9 L263-265. Ref [26] has been added.

3) the fluctuation of normalized peak areas in Figure 1B (peaks B and C) with the time is difficult to understand and the hypothesis provided is not convincing at all (aggregation kinetic versus experimental time points as well as peak shape of peak B and C)

However difficult it may be to understand, this is what we indeed observe for 5 independent experiments, for which we produce SD of normalized peak areas. At P11 L319-324 we comment the puzzling peak shape of peak C and we produce pieces of evidence to rule out that this peak may be an electric spike.

4) the peptide concentration is really high compared to what can be expected in vivo; this also may have a significant impact on oligomerization process.
It is well known that kinetics of aggregation is strictly dependent on several factors, including peptide concentration. In general, the higher the peptide concentration the faster the aggregation kinetics. In this work, the concentrations used are comparable to those used by many authors for in vitro Aß aggregation experiments. See, as examples refs already included in reference list [15, 20, 37].

5) could the first peak observed in Figures 1 and 2 considered as the monomeric form?
No, as evident from UF results in Figure 4d), relevant to peaks observed in Figure 1. As far as Figure 2, no characterization was carried out as already explained in text (P12 L353-355).

6) it is not clear what the UV spectrum can bring to the analysis.
The UV absorbance rules out the assignment of an electric spike to this sharp peak. A similar spectrum is obtained for all other peaks present in the electropherograms (data not shown).
See also reply on DAD spectrum to reviewer #1. The sentence at P11 L321-322 has been completed.

7) variability between batches and between providers seems to be very important. How can it be explained on a small amyloid peptide.
This is an enormous issue that it is often underestimated or disregarded, as already pointed out in text. The only scope of this manuscript is to bring it to light. We do not attempt any explanation, as so far it is difficult to find a rule among the variabilities observed. Constant communication with suppliers does not help.

8) viability test (MTT test) realized with the different fractions bigger or lower than 50 kDa are very interesting but did the authors stimulated the cells with the same peptide concentration in all conditions?
As already reported at P8 L243 "..cells were exposed to approximately 10 µM entire Aß42 peptide (prepared according to protocol #3) for 24 h at 37°C or to filtrated and retained solutions obtained after ultrafiltration experiments..". As already reported

at P10 L308-310 "Because standards are not available, a quantitative evaluation of the oligomers observed in CE is intrinsically unaccessible."

At P6 L179-182 it is already reported that 50kDa membranes reverse spinning is feasible and therefore recovery of the retained portion is more reliable (Figure 4b). In our opinion these statements altogether make the reply to this question

Are the replicates independent?

Yes, the replicates are independent, as already reported at P8 L244.

Indeed, SD are anomaly small.

It might not have been resulted clear that we expressed precision with standard error of means (SEM) in Figure 6 and with means ± SD in text. To avoid any misunderstanding, we now produce precision data as mean ± SD both in text (P16 L497, 502), Figure 6 and its caption.

***Novelty Statement**

As compared with previous work, this manuscript focuses on the effect that different Aß42 sample preparation protocols have on the formation of assemblies in solution; experimental conditions are finely tuned so to considerably extend the time window over which these oligomers are soluble and to obtain unprecedented reproducible results.

Not only does this approach enable an easier isolation of the separated species by ultrafiltration and the assignment of their cell toxicity, but also it makes possible for the first time an independent analysis of the secondary structure of the same species by ATR-FTIR.

Finally, it is shown how a simple CE analysis of Aß42 can shed light on a crucial issue whose importance is hardly ever addressed: peptide batch-to-batch and supplier-to-supplier reproducibility.

***Highlights (for review)**

- Aß oligomers are identified and characterized by a standardized analytical platform
- CE provides information on the reproducibility of Aß42 sample preparation protocols
- ATR-FTIR corroborates characterization performed in solution by ultrafiltration
- Monomers up to hexamers of Aß42 are not toxic
- CE detects supplier-to-supplier variability of Aß42 aggregation

AN INTEGRATED STRATEGY TO CORRELATE AGGREGATION STATE, STRUCTURE AND TOXICITY OF Aß 1-42 OLIGOMERS.

Federica Bisceglia [a], Antonino Natalello [b], Melania Maria Serafini [a,c], Raffaella Colombo [a], Laura Verga [d], Cristina Lanni [a], Ersilia De Lorenzi [a]

[a] Department of Drug Sciences, University of Pavia, Viale Taramelli 12, 27100, Pavia, Italy.

[b] Department of Biotechnology and Biosciences, University of Milano Bicocca, Piazza della Scienza 2, 20126, Milano, Italy.

[c] Scuola Universitaria Superiore IUSS Pavia, Piazza della Vittoria 15, 27100, Pavia, Italy.

[d] Unit of Pathology, IRCCS Policlinico S. Matteo Foundation and University of Pavia, Via Forlanini 14, 27100, Pavia, Italy.

Corresponding author:

Prof. Ersilia De Lorenzi,

Department of Drug Sciences, University of Pavia, v.le Taramelli 12, 27100, Pavia.

email: ersidelo@unipv.it

tel +39 0382 987747

fax +39 0382 422975

Keywords: Alzheimer's disease; Capillary electrophoresis; Aß 1-42; Aß oligomers; Sample preparation; Fourier transform infrared spectroscopy.

Abbreviations: Aß, Amyloid-beta; Aß42, Aß 1-42; CE, capillary electrophoresis; AD, Alzheimer's disease; TEM, transmission electron microscopy; ATR-FTIR, Attenuated total reflection-Fourier transform infrared; FSD, Fourier self deconvolution; EOF, electroosmotic flow.

ABSTRACT

Despite great efforts, it is not known which oligomeric population of amyloid beta (Aß) peptides is the main neurotoxic mediator in Alzheimer's disease. *In vitro* and *in vivo* experiments are challenging, mainly because of the high aggregation tendency of Aß (in particular of Aß 1-42 peptide), as well as because of the dynamic and non covalent nature of the prefibrillar aggregates. As a step forward in these studies, an analytical platform is here proposed for the identification and characterization of Aß 1-42 oligomeric populations resulting from three different sample preparation protocols. To preserve the transient nature of aggregates, capillary electrophoresis is employed for monitoring the oligomerization process in solution until fibril precipitation, which is probed by transmission electron microscopy. Based on characterization studies by ultrafiltration and SDS-PAGE/Western Blot, we find that low molecular weight oligomers build up over time and form bigger aggregates (> dodecamers) and that the kinetics strongly depends on sample preparations. The use of phosphate buffer results to be more aggregating, since trimers are the smallest species found in solution, whereas monomers and dimers are obtained by solubilizing Aß 1-42 in a basic mixture. For the first time, attenuated total reflection-Fourier transform infrared spectroscopy is used to assign secondary structure to the separated oligomers. Random coil and/or α-helix are most abundant in smaller species, whereas ß-sheet is the predominant conformation in bigger aggregates, which in turn are demonstrated to be responsible for Aß 1-42 toxicity.

1. INTRODUCTION

It is estimated that more than 30 million people worldwide suffer from Alzheimer's disease (AD) [1]. The evidence that different molecular pathways are involved in neurodegeneration makes AD a multifactorial disease [2] and this explains the difficulties in defining the aetiology and in discovering effective treatments [1, 3]. Among many factors, it is now well established that the soluble aggregates of amyloid-beta (Aß) protein play a crucial role in the onset of the disease and therefore studying their self-assembly is the focus of intense research. Aß protein is a family of peptides that ranges from 36 to 43 amino acids and derives from the proteolytic cleavage of the amyloid precursor protein (APP) [4]. Unfolded or partially folded Aß monomers interact through a nucleation-elongation process to form small oligomers and nuclei that rapidly lead to larger aggregates and then to fibrillar forms [5, 6]. In turn, the insoluble amyloid fibrils deposit in the brain as extracellular amyloid plaques which represent one of the two hallmarks of AD, together with neurotangles of hyperphosphorylated tau protein [1, 5]. In the last two decades the soluble pre-fibrillar oligomers of Aß peptides have been recognised as the principal neurotoxic mediators which lead to detrimental effects on the AD brain [3, 7, 8]. Despite significant efforts, the structure of these Aß oligomers, the understanding at the molecular level of their aggregation process, the exact mechanism of oligomer-induced toxicity as well as the accurate identification of the neurotoxic oligomeric species, remain elusive. Intrinsic limitations in investigating Aß oligomers are mainly related to their peculiar nature: they consist of heterogeneous populations of polymorphic, non-covalent and transiently populated aggregates generated by multiple pathways. This is true especially for Aß 1-42 (Aß42), which is the most amyloidogenic and toxic among the Aß peptides [3, 8, 9].

Important progress has been made through *ex vivo* and *in vitro* studies performed either with AD brain-derived oligomers or synthetic peptides. Because of the target organ of amyloid aggregates, the availability of brain-derived species is clearly restricted and *ex vivo* studies are difficult to approach [9, 10]. In principle, by using synthetic peptides a strict control of the starting material and a modulation of the aggregation process could be achieved, even if exact physiological conditions cannot be replicated. On the other hand, because of their high aggregation tendency, and in particular that of Aß42, a fine tuning of the oligomer formation and kinetics is challenging. Each specific solubilization protocol (different solvents, peptide concentrations, incubation time and temperature) leads to different oligomeric species [11, 12]. Notably, authors very often claim the presence in solution of aggregates of defined size on the basis of previous literature data that report the same or similar sample preparation. In this specific context it is easy to make wrong assumptions, also because synthetic peptides are characterized by extreme variability including supplier-to-supplier and batch-to-batch, an issue that is rarely addressed [13]. These limitations, together with the complex dynamic equilibrium existing among Aß species contribute to the widespread and controversial literature on Aß oligomers [3, 9].

Complementary information on the isolation and size estimation of Aß aggregates and the related toxicity has been achieved over the years by multiple techniques such as SDS-PAGE [8, 14] size exclusion chromatography (SEC) [15], dynamic and multiangle light scattering (DLS and MALS) [15, 16], microscopy [5], mass spectrometry [17], NMR spectroscopy and X-ray crystallography [18]. Each technique is not devoid of limitations and drawbacks. These are mainly related to the non covalent and dynamic nature of Aß oligomers and to the ability of a technique to provide information on small and large oligomers with an equivalent accuracy. For example, DLS and MALS can not intrinsically separate different oligomeric populations for independent characterization [3, 10]; fluorescence-based detectors require non-native labelled peptides that may alter the oligomerization kinetics [19]; both MALDI and ESI ionization sources may induce oligomer dissociation[20]. Some authors successfully stabilized the transient nature of oligomers by photo-induced cross-linking, to analyze the resulting "frozen" oligomers by SEC or SDS-PAGE [8]. While this procedure overcomes the dissociation induced by e.g. SDS-PAGE, it also implies that oligomers do not exactly mirror the native state in solution.

The use of capillary electrophoresis (CE) with UV detection to monitor *in vitro* Aß oligomer formation was pioneered by our group [21]. CE works in free solution and in the absence of a stationary phase or chaotropic agents, thus it preserves the native oligomeric structure and provides a real time snapshot of different soluble and unlabelled Aß assemblies during their formation.

Over the years CE-UV was employed to detect and separate soluble oligomeric species of Aß peptides ranging from monomers [22-25] to aggregates larger than dodecamers [21, 22, 26-28]. To provide oligomer size characterization, CE separation was also used concurrently with Taylor dispersion analysis [22], ultrafiltration [21, 26-28], MALDI-TOF [25] and very recently electrospray differential mobility analysis [23]. In these works the CE separation is limited to two main oligomeric populations that are rapidly precipitating and for which a dynamic equilibrium is often not demonstrated. Here instead we initially focus on the effect that different Aß42 sample preparation protocols have on the formation of assemblies in solution; experimental conditions are finely tuned so to obtain and separate by CE as many oligomeric populations as possible and to considerably extend the time window over which these oligomers are soluble. Not only does this approach enable an easier isolation of the separated species by ultrafiltration and the assignment of their cell toxicity, but also it makes possible for the first time an independent analysis of their secondary structure by attenuated total reflection-Fourier transform infrared (ATR-FTIR) spectroscopy. Finally, it is shown how a simple CE analysis of Aß42 can shed light on a crucial issue whose importance is hardly ever addressed: peptide batch-to-batch and supplier-to-supplier reproducibility.

2. MATERIALS AND METHODS

2.1 Materials

Synthetic Aß42 (MW 4514.10 Da) was purchased as lyophilized powder from Anaspec (Fremont, CA, USA), (purity ≥ 95%; lots #1556608, #1556609, #1457203) and Bachem (Bubendorf, Switzerland), (purity ≥ 95%; lots #10533163, #1065556, #1056654) and stored at -20°C. 1,1,1,3,3,3-Hexafluoropropan-2-ol (HFIP), dimethylsulfoxide (DMSO), acetonitrile (ACN), and sodium carbonate were from Sigma-Aldrich (St. Louis, MO, USA). Sodium hydroxide and sodium dodecyl sulphate (SDS) were provided by Merck (Darmstadt, Germany). Na_2HPO_4 and NaH_2PO_4, supplied by Sigma-Aldrich, were used for the preparation of the background electrolyte (BGE) in the CE analyses. BGE solutions were prepared daily using Millipore Direct-Q™ deionized water (Bedford, MA, USA) and filtered with 0.45 µm Sartorius membrane filters (Göttingen, Germany).

Ultrafiltration devices (10, 30 and 100 kDa cutoff) were purchased from Pall Corporation (New York, NY, USA), whereas 50 kDa cutoff membranes were from Millipore (Billerica, MA, USA).

The 3-(4,5-dimethylthiazol-2-yl)-2,5-diphenyl-tetrazolium bromide (MTT) and phosphate buffered saline (PBS) employed in the cell viability assay were supplied by Sigma-Aldrich.

2.2 Solubilization protocols

Aß42 oligomers were prepared by following three different solubilization protocols.

Protocol #1: Aß42 (Anaspec) was solubilized in HFIP (1 mg/mL, ~ 221 µM). The stock solution was gently mixed and then kept for 30 minutes at 4°C, aliquoted in microfuge tubes and lyophilized via Speed-Vac. Then Aß42 aliquots were redissolved in 20 mM Na_2HPO_4/NaH_2PO_4, pH 7.4.

Protocol #2: Aß42 (Anaspec) aliquots were prepared as in #1 and then redissolved in DMSO/20 mM phosphate buffer (pH 7.4) at increasing concentrations of DMSO.

Protocol #3: Aß42 (Bachem) was prepared as described by Bartolini *et al* [29]. Briefly, the peptide was solubilized in HFIP (149 µM) and kept at room temperature overnight. The stock solution was aliquoted in microfuge tubes and kept at room temperature for one day, then HFIP was left to evaporate overnight. The resulting peptide film was redissolved to obtain 500 µM Aß42: the redissolution mixture consisted of ACN/300 µM Na_2CO_3/250 mM NaOH (48.3:48.3:3.4, v/v/v). The final peptide solution (100 µM) was obtained by the dilution of 500 µM Aß42 with 20mM Na_2HPO_4/NaH_2PO_4 (pH=7.4).

For all protocols final solutions were not centrifuged, to avoid mechanical stress at the beginning of the aggregation process.

2.3 Capillary electrophoresis and ultrafiltration

Aß42 samples were analyzed by CE at different elapsed times from t0, where t0 is defined as the time when the HFIP-lyofilized peptide is redissolved.

CE analyses were performed on an Agilent Technologies 3D CE system (Waldbronn, Germany) equipped with a diode-array detector (DAD) set at λ=200 nm. Data were collected using Chemstation A.10.02 software.

In the present work, two CE methods (A and B) were applied. Uncoated fused-silica capillaries provided by Polymicro Technologies (Phoenix, AZ, USA) were pretreated by flushing 1 M NaOH, deionized water and BGE (80 mM sodium phosphate buffer, pH=7.4) for 60 min, 60 min and 90 min (method A), or for 30 min, 30 min and 60 min (method B), respectively. BGE was prepared by mixing 80 mM solutions of Na_2HPO_4 and NaH_2PO_4 in order to obtain the desired pH.

In method A [28] the analytical separation was carried out at 16 kV (current: 75-80 µA) on a capillary of 53 cm of total length (L=53 cm, l=44.5 cm). Samples were hydrodynamically injected by applying 50 mbar for 8 s. In method B, a capillary of L=33 cm, l= 24.5 cm was used; the applied voltage was 12 kV (current 75-80 µA) and hydrodynamic injection parameters were set at 30 mbar for 3 s. For both methods the capillary temperature was 25°C and the between-run rinsing cycle consisted of 50 mM SDS (1.5 min), deionized water (1.5 min), and BGE (2 min).

The electroosmotic flow (EOF) is easily measured as a perturbation of the baseline given by solvents used for the redissolution of the lyophylized Aß42 aliquots and thus it is considered as a reliable noninteracting marker. The effective mobilities (μ_{eff}, $cm^2V^{-1}s^{-1}$) of each peak are calculated by subtracting the contribute of the EOF (μ_{EOF}) from the apparent mobility (μ_{app}, $cm^2V^{-1}s^{-1}$). Semiquantitative analyses were performed based on the normalized area % [30]. Aß42 peptide solutions were ultrafiltrated on devices at different elapsed times from t0 and the resulting filtrated and retained solutions were analyzed by CE. Ultrafiltration experiments were carried out in triplicate and by applying the best experimental conditions for each type of membrane, as suggested by suppliers: 14000 g for 10 minutes with 10, 30, and 100 kDa cutoff membranes and 60 minutes with 50 kDa cutoff membranes. In order to obtain enough volume of the retained solutions and to approximately restore the original concentration, a volume of 20 mM phosphate buffer (pH 7.4), equal to that of the ultrafiltrated sample, was added to the retained portion that was recovered by reverse spinning (14000 g, 5 minutes, for 50 kDa membrane). For 10, 30 and 100 kDa devices, since the reverse spinning is not intrinsically possible because of their geometry, the retained portion was recovered by using a micropipette.

Appropriate quantification of the retained sample amount is clearly not possible. However, the comparison of the electropherograms obtained before and after ultrafiltration was used to verify that the concentrations of the injected species were qualitatively comparable.

2.4 Transmission electron microscopy

Precipitated samples were fixed on carbon-coated Formvar nickel grids (200 mesh) (Electron Microscopy Sciences, Washington, PA, USA). Aß42 suspensions were diluted to 10 µM with 20 mM phosphate buffer (pH 7.4). Ten µL suspension were left to sediment on grids; after 15 minutes the excess of sample was drained off by means of a filter paper. The negative staining was performed with 10 µL of 2% w/v uranyl acetate solution (Electron Microscopy Sciences). Sample investigations were carried out in triplicate by using a JEOL JEM 1400-Plus electron microscope, operating at 80 kV (Peabody, MA, USA).

2.5 Fourier Transform Infrared spectroscopy

Structural properties of Aß42 solubilized by protocol #1 and protocol #3 and those of filtrated and retained solutions on 50 kDa cutoff membrane were analyzed by FTIR measurements in attenuated total reflection (ATR) [31-34]. For these analyses, 2 µl of each sample were deposed on the single reflection diamond crystal of the ATR device (Quest ATR, Specac, Orpington, UK). In order to obtain a hydrated peptide film, samples were dried [31] at room temperature.The ATR-FTIR spectra of the hydrated films were recorded by a Varian 670-IR spectrometer (Varian Australia Pty Ltd, Mulgrave VIC, Australia), which was continuously purged with dried air. Conditions applied were: 2 cm^{-1} resolution, scan speed of 25 kHz, 1000 scan coadditions, triangular apodization, and a nitrogen-cooled Mercury Cadmium Telluride detector [34]. The measured spectra were normalized at the area of the Amide I band (around 1700-1600 cm^{-1}) to compensate for possible differences in the peptide content. Fourier self deconvolution (FSD) was obtained with a full width at half height of 13.33 cm^{-1} and a resolution enhancement factor K = 1.5. Spectral collection, the FSD and the second derivative analyses [33] were performed using the Resolutions-Pro software (Varian Australia Pty Ltd). The evaluation of the peptide secondary structures was obtained by curve-fitting of the FSD spectra in the Amide I spectral region [31, 33]. Because the result of this procedure is not unique, the selection of the input parameter is very important. Here a linear baseline was employed and the number and peak position of the initial components were taken from the second derivative and FSD spectra. Curve-fitting was performed by leaving the initial parameters (baseline, peak position, band width, and band intensity) free to adjust iteratively with the only exception of the two Amide I components assigned to β-sheet structures (around 1633-1628 cm^{-1} and around 1695-1692 cm^{-1}, respectively [31, 33]), whose positions were restricted within 4 cm^{-1} from the wavenumbers observed in the second derivative spectra. The same set of input parameters were employed for the curve-fitting of the FSD spectra of the different Aß42 preparations, to allow a more reliable evaluation of the differences in the secondary structure content among the analyzed samples. The curve-fitting was performed using the GRAMS/AI 8.0 software (Thermo Electron Corporation, Waltham, USA).

In control experiments, the same Aβ42 preparations were measured in ATR without solvent evaporation [33]. For these analyses, 20 µl of each sample were deposed on the nine-reflection diamond crystal of the ATR device (DuraSamplIR II, Smith Detection, USA) and the ATR-FTIR spectra were immediately collected as described above. The peptide spectra were obtained after subtraction of the buffer contribution and analysed following the same procedures employed for the peptide film spectra.

2.6 SH-5YSY cell viability assay

SH-SY5Y human neuroblastoma cell cultures (ECACC No. 94030304) were grown at 37°C in 5% CO_2/95% air in a medium composed of Eagle's minimum essential medium and Nutrient Mixture Ham's F-12, with the addition of 10% FBS, 2 mM glutamine, penicillin/streptomycin, non essential amino acids. All culture media and supplements were purchased from Euroclone (Life Science Division, Milan, Italy).

The MTT colorimetric assay based on the reduction of MTT by mitochondrial dehydrogenase was employed to evaluate the cellular redox activity as initial indicator of cell death. At day 0, SH-SY5Y cells were plated at a density of $5x10^4$ viable cells *per* well in 96-well plates. The next day, cells were exposed to approximately 10 µM entire Aß42 peptide (prepared according to protocol #3) for 24 h at 37°C or to filtrated and retained solutions obtained after ultrafiltration experiments and then to a MTT solution in PBS (1 mg/mL). After 4 h incubation, cells were lysed with lysis buffer (20% SDS in water/dimethylformamide 1:1) and incubated overnight at 37°C. The cell viability reduction was quantified by using a Sinergy HT microplate reader (Biotek, Winooski, Vermont, USA).

For statistical analysis the GraphPad Instat statistical package (version 3.05 GraphPad software, San Diego, CA, USA) was used. Data were analyzed by analysis of variance (ANOVA) followed, if significant, by an appropriate post hoc comparison test. The reported data are expressed as mean ± standard deviation (SD) of three independent experiments. Values of $p<0.05$ were considered statistically significant.

3. RESULTS AND DISCUSSION

3.1 Monitoring of Aß42 aggregation process by CE

Both small and large oligomers seem to exert neurotoxicity and also the ongoing polymerization process may be responsible for Aß toxicity and neurodegeneration in AD [6, 9].

Over the years increasing attention has been paid towards small oligomers deemed to be toxic such as monomers, dimers, trimers, tetramers, nonamers and dodecamers [14, 17, 35, 36].

Therefore, aim of this work is also to promote the formation of low MW species and to demonstrate the existing dynamic equilibrium by keeping the formed assemblies soluble for a wide time window. In this way we intend to overcome the limitations very often shown by existing CE-based experiments: data obtained on short-lived (i.e. rapidly precipitating) samples, separation of two main oligomeric populations only [23, 25, 28], lack of properly replicated data over a defined time frame, little or no characterization of the separated species and of the final precipitates.

The outline of the sample preparation protocols is reported in Figure S1. The three procedures share an initial treatment with HFIP then, depending on the degree of aggregation required, different solvents have been employed. As demonstrated by circular dichroism and atomic force microscopy data [29, 37], fluorinated alcohols like HFIP are able to promote α-helix conformation and disrupt ß-sheet structures, thus erasing the "structural history" of Aß42 [12].

Notably, in all experiments we kept the operative current value very similar to that reported in [21, 26] so as to ensure that the electric field does not influence the strength of the noncovalent intermolecular interactions that sustain the peptide oligomerization, as demonstrated in [21].

3.1.1 Protocol #1

The dried film obtained after lyophilization of the HFIP-solubilized peptide is redissolved in phosphate buffer at physiological pH, to trigger the formation of aggregates. In general, salts dissolved in aqueous solutions have an important role in promoting protein-protein association. Salts can reduce repulsive electrostatic interactions through an increase of the apparent dielectric constant of water and can interact with charged or polar residues thus stabilizing salt bridges [38, 39]. Because of specific interactions with Aß histidine residues, phosphate ions have been reported to strongly affect the fibrillogenesis and oligomerization of amyloid peptides [40].

Figure 1a) shows a selection of CE traces of the same peptide sample when injected at different elapsed times from t0. Electropherograms are representative of one out of five independent experiments.

Conversely to what reported in previous work by us [21, 26-28] and sometimes by others [22, 41], this sample preparation affords detectable soluble species over a time window which is up to more than 10 folds longer, before precipitation. Given the very high aggregation tendency of Aß42, the likely presence of insoluble material in the solutions used in many experiments affects data reproducibility and accuracy and,

obviously, also aggregation kinetics and toxicity data. Declaration and demonstration of the time span over which the prepared sample is soluble is rarely found and nevertheless it is mandatory, if sound results have to be produced. In this respect, a technique that works in free solution such as CE is an asset, as the presence of in-capillary insoluble material, adhesion phenomena and unwanted interactions with the capillary wall are easily spotted by spikes in the electropherogram, current fluctuations or dropping, irreproducible migration times and peak areas.

In Figure 1a) three peaks are separated. Notably, the effective mobilities (μ_{eff} values) are averaged on 10 monitoring times from 5 independent experiments, using three different peptide batches from the same supplier (Anaspec). The excellent RSD% values allow peak labelling as A, B and C all the way through the monitoring time, on the basis of precise electrophoretic mobilities. Conversely to what reported by using different [21, 26-28] or similar [25] sample preparations, Figure 1a) reveals that, already immediately after redissolution of the dried film, the earlier migrating peak A is the most abundant and aggregation has already started, as two more peaks are present.

Transmission electron microscopy (TEM) image taken at t0 in Figure 1a), representative of three independent experiments, reveals that also fibrils are present in this sample: as the solution is neither stirred nor centrifuged before analysis, it is likely that they are sedimented at the bottom of the anodic vial and thus they are not injected into the capillary, as confirmed by the absence of spikes in the electropherogram. Since oligomers and fibrils are at equilibrium in the brain [9] this protocol better mimics *in vivo* conditions, as compared to protocols that force the apparent formation of monomers [22].

According to our previous work [21, 26-28], and following the hypothesis that mass prevails over charge in the migration observed, it is plausible to anticipate that the faster migrating population corresponds to low MW oligomers (peak A), whereas peaks B and C should be higher MW species. Bearing in mind this hypothesis and as a preliminary investigation, four solutions injected in CE (at t0, 5.5 h, 81 h and 5 days) have been analyzed by SDS-PAGE/Western Blot (Figure S2). Bands ranging from dimers up to 22-mers are detected. Contrary to CE data, bands relative to large oligomers are observed in WB analyses only at a late stage of the aggregation process. Further, bands corresponding to Aß42 dimers up to tetramers are abundant even at 81 h and 5 days, when the electrophoretic peak A has already totally converted into larger aggregates.

Because standards are not available, a quantitative evaluation of the oligomers observed in CE is intrinsically unaccessible. Notwithstanding this limitation, a CE semi-quantitative analysis based on normalized peak area percent [30] is carried out in triplicate: for each monitoring point, SD is lower than 9%. In Figure S3a) (Supplementary material), the normalized areas over the entire time span are provided, and in Figure 1b), a focus on the early aggregation times up to 72 hours can be found. Altogether, it is clear that with the progression of the self-assembly process, the putative small oligomers (peak A) are depleted and contribute to the formation of peaks B and C, possibly corresponding to larger species. At later times

only peak C is detected. More in detail, peaks B and C are at mutual equilibrium within the first 72 hours: the area of peak B increases and that of peak C decreases and vice versa. This could be well one of the several equilibria hypothesized among oligomers [3, 9], that is kept inside the capillary where species are free to interconvert. The observation of a sharp and efficient peak (peak C) after a broad band such as peak B, may suggest ongoing precipitation and the presence of a spike [22, 25, 41]. However, three pieces of evidence rule out this hypothesis: i) the dynamic equilibrium between peak B and peak C; ii) the high reproducibility of peak C mobility; iii) the UV spectrum taken by DAD detector, similar to that obtained for the other peaks relative to Aß peptide (Figure S3b)). At the end of the aggregation process no more peaks are detected by CE, the sample is visibly cloudy and the TEM analysis of the resuspended precipitate reveals the presence of fibrils (Figure 1 a)).

3.1.2 Protocol #2

DMSO is a highly polar, water-miscible organic solvent which is also commonly used to solubilize Aß peptides. In a vast majority of toxicity studies on cells, highly concentrated Aß (e.g. 5 mM) is dissolved in 100% DMSO and then diluted with PBS [42] or in cell culture medium [12]. Its effect on aggregation is very controversial. Some studies have demonstrated that Aß40 and Aß42 in pure DMSO remain stable in a monomeric α-helical structure and give rise to the so called "unaggregated Aß peptides preparations", or "unaggregated fibril-free preparations" [12, 43], since DMSO prevents the organization of Aß in ß-sheet structures by hindering the formation of hydrogen bonds [12, 37, 44]. Other experiments instead clarified that 100% DMSO is not sufficient to maintain a monomeric solution [37]. Finally, other papers reported that when pure DMSO is diluted with buffer or water, it can immediately induce the formation of oligomeric aggregates and protofibrils [12, 37]. To shed light on these controversial data, in protocol #2 (Figure S1) either pure or phosphate buffer-diluted DMSO is used as redissolution solvent of the HFIP-dried film. As compared to protocol #1, protocol #2 is intended to obtain smaller oligomeric populations or even a single homogeneous monomeric population. The addition of 20% DMSO to Aß42 samples does not affect CE profiles and oligomerization, as compared to the results in Figure 1 a) (data not shown). By addition of either 50% or 100% of DMSO the aggregation process is comparable, thus in Figure 2 only results obtained with 100% DMSO as solubilizing solvent are reported. Peaks are labelled as in the electropherograms of Figure 1 a), because they are identified on the basis of statistically equal electrophoretic mobilities, therefore it is plausible to hypothesize that the size distribution is similar. Peaks A, B and C are detected together with other minor species.

Conversely to what claimed by Stine *et al.* in a seminal work [37], here the electropherogram at t0 clearly indicates that sample preparation using HFIP and then pure DMSO does not produce a single, uniform and unaggregated sample. The use of DMSO as solubilizing agent ensures a longer time window where

oligomers are kept soluble if compared to that obtained by following protocol #1; in particular, the first migrating population (peak A) is detected at very long times after redissolution. However, neither are fibrils present immediately after solubilization nor at the end of the process: Aß42 prepared according to protocol #2 precipitates as amorphous aggregates after about one month from t0. This could explain also the observed absence of dynamic equilibrium between oligomers (Figure S4). Another limitation that hinders any further investigation is that the CE data obtained feature a DMSO concentration that is not only toxic for neuroblastoma cells but also chemically incompatible with ultrafiltration devices.

3.1.3 Protocol #3

By preparing the sample according to protocol #1 multiple equilibria are observed by CE, i.e. that between faster (peak A) and slower (peaks B and C) migrating species and that between the putative bigger assemblies (peak B and peak C). However, the putative small oligomers rapidly contribute to the formation of large aggregates by progressively decreasing peak A area, so that little information about smaller species is obtained.

In order to shift the aggregation process further towards low molecular weight oligomers, Aß42 was solubilized following a protocol previously set up [29]. To accurately replicate what reported by Bartolini *et al.* the peptide here used was purchased by the same supplier (Bachem). After preparing the sample according to this protocol (here defined as protocol #3, Figure S1), Aß42 is injected in CE and its self-assembly is monitored over time by an optimized CE method (method B). This method considerably shortens analyses times (less than 7 min), in turn it allows more frequent sampling and improves efficiency. By a multimethodological approach, in [20] authors demonstrated and/or inferred the formation of assemblies ranging from monomers up to decamers immediately after solubilization, and of higher MW oligomers including protofibrils within the first 12-48 hours, before sample precipitation.

In Figure 3a) it is clear that at t0 the sample already includes at least three main electrophoretic peaks as well as amyloid fibrils, which are observed by TEM. That protocol #3 is less aggregating than the first protocol is also evident: soluble species are detected for longer times, including two earlier migrating and very narrow peaks. This could be explained by the longer contact of lyophilized Aß peptide with HFIP and by the treatment with a basic mixture in ACN, so to keep a non amyloidogenic conformation [29].

In Figure 3a), mobilities are calculated as average of 5 independent experiments using three peptide batches from the same supplier. Effective mobilities are statistically different from those reported in Figure 1a), except for those of the fastest migrating peak, where values fall within the experimental errors, equal to two times the standard deviation [45]. However, they are labelled as peak 1, 2 and 3.

Analogously to what shown by others [22] minor species are also visible and nevertheless they are not taken into consideration in this study, given the low abundance and the absence of dynamic equilibrium. From electrophoretic traces Figure 3a) and from the graph in Figure 3b) it emerges that the faster migrating population consists of two peaks at dynamic equilibrium: peak 1 slowly contributes to the formation of peak 2. As for protocol #1, the reproducibility of the normalized area percent is very good (SD < 8%). A progressive reduction of both peaks 1 and 2 area is observed, while a slower migrating broad band (peak 3) is built up. Therefore, as compared to protocol #1 (Figure 1), the aggregation is slowed down to such an extent that an equilibrium among the putative small species is appreciable by CE. Aß42 oligomers are soluble for about one month until precipitation into amyloid fibrils.

An issue that is rarely raised by authors who report studies on Aß42 is the very high variability of commercial peptides with regard to solubility and in turn aggregation properties. To our knowledge, a single systematic study on different Aß42 suppliers, however limited to the effect on fibril polymorfism, was reported [13].

In particular methods of synthesis and purification could be source of variability. Notably, batch-to-batch variations in the declared degree of purity may be found, as well as different instructions for standard peptide solubilization within the same supplier and among different suppliers. In our experience this problem can not be neglected and this is the reason why, to support their robustness, all CE data are here averaged on different batches purchased from the same supplier.

Notably, when Aß42 supplied by Anaspec is solubilized according to protocol #3, it shows the same electrophoretic profile of the Bachem peptide (data not shown). Conversely, when Aß42 provided by Bachem is solubilized by following protocol #1, precipitation occurs after 30 minutes from t0, when soluble species are not detected, the sample is visibly cloudy and TEM analysis shows fibrils (Figure S5). These data confirm the high variability of synthetic peptides and suggest that a given protocol cannot be applied to any purchased peptide standard but it strongly depends on the supplier. Therefore it is imperative to have a tool suitable to verify peptide solubility.

3.2 Aß42 oligomer characterization

3.2.1 CE analyses of ultrafiltrated samples

Highly reproducible CE analyses of soluble oligomers over a wide time window are the necessary premises for a reliable characterization of the separated species.

In order to assign a range of MW to the oligomers analytically separated by CE and prepared by protocols #1 and #3, ultrafiltration experiments are carried out with different cutoff membranes. Solutions to be ultrafiltrated have been selected at appropriate elapsed times from solubilization, depending on the

favourable relative abundance of the peak areas observed in CE. In principle ultrafiltration is not devoid of limitations, as it can only assign a molecular weight range and adsorption phenomena may affect sample recovery and data interpretation. Nevertheless this approach is very simple, fast, and CE analyses serve as a control of the oligomeric state, by comparison between unfiltered, retained and filtrated solutions. In general, it is reasonable to consider that, while the amount found in filtrated solutions has to be entirely ascribed to actual filtrated protein material, the amount found in the retained solution can partly be constituted by aggregated peptide adsorbed on the filter and not necessarily retained in virtue of its size. Oligomers ranging from trimers up to dodecamers migrate under peak A (protocol #1): peak A is totally retained on 10 kDa (Figure 4d)), mostly on 30 kDa (Figure 4 c)) and filtrated through 50 kDa membrane (Figure 4 b)). Based on these evidences, the bands corresponding to Aß42 dimers detected by SDS-PAGE/Western Blot (Figure S2) must definitely be ascribed to an artefact due to oligomer disaggregation induced by SDS: as seldom reported [14, 46], it can be concluded that SDS-PAGE, despite its widespread usage, does not mimic the actual conditions in solution. The slower migrating peaks B and C correspond to aggregates smaller than 22-mers and larger than dodecamers, since they are quantitatively recovered in the filtrated solution of 100 kDa cutoff and in the retained solution of 50 kDa cutoff (Figure 4 a) and b)), respectively.

Along with what stated for peaks B and C and based on membrane specifications, ultrafiltration on 50 and 100 kDa membranes (Figure 4 a) and b)) shows that peak 3 corresponds to aggregates larger than dodecamers and that no aggregates bigger than 100kDa (22-mers) are present in solution. Considering the low recovery of peak 3 in the filtrated solution, it is assumed that part of the peptide is entrapped in the filter. On the other hand, the size distribution of small assemblies is different from protocol #1. Identification of peaks 1 and 2 a from monomers up to hexamers is revealed by electropherograms of samples filtrated on 10 and 30 kDa membranes (Figure 4 d) and c)).

Membrane specifications for 30 kDa and 10 kDa devices make us reasonably hypothesize that peaks 1 and 2 correspond to monomers and dimers, respectively. By simple ultrafiltration experiments the presence of monomers and dimers in solution, as demonstrated in [20], is confirmed. It is valuable that in this work the presence of soluble Aß oligomers is monitored for much longer time

3.2.2 ATR-FTIR characterization of the secondary structure of Aß42 oligomers

The conformational features of the different Aß42 oligomers obtained by protocol #1 and protocol #3 were investigated by ATR-FTIR spectroscopy. This approach provides information on the peptide secondary structures and intermolecular interactions through the analysis of the Amide I band (around 1700-1600 cm^{-1}) manly due to the stretching vibration of the C=O peptide group [32, 33, 47]. Figure 5a) shows the FSD spectra of the peptide films of Aß42 solubilized by protocol #1 (at 2.5 h) before and after ultrafiltration through a 50 kDa cutoff membrane. The spectra of the whole peptide and of the retained assemblies are

characterized by an intense peak around 1630 cm^{-1} and by a minor component around 1695 cm^{-1}, both assigned to ß-sheet structures [31]. The intensity of the ~1630 cm^{-1} component decreases in the filtrated solution indicating a lower ß-sheet content in this sample (Figure 5a)). The intensity ratio 1695/1630, called ß-index, has been suggested to be proportional to the percentage of antiparallel ß-sheet in the structure and has been widely employed in the FTIR analyses of Aß and other amyloidogenic polypeptides [32]. The ß-index values calculated from the baseline corrected FSD spectra of Aß42 solubilized by protocol #1 (Figure 5b)) are within the range expected for Aß peptide oligomers with a predominantly antiparallel organization of the ß-sheets [31, 32, 48]. For a semi-quantitative comparison of the ß-sheet content in the different samples, a curve-fitting analysis on the FSD spectra was performed (Figure 5c) and Figure S6-FTIR1). The entire peptide preparation and the retained solution are characterized by a higher amount of ß-sheets (average ± SD: 62.74% ± 4.87 and 66.76% ± 1.68, respectively) as compared to that of the filtrated solution (48.60% ± 3.31). These findings are in agreement with the characterization obtained by ultrafiltration (Figure 4 b)) and mirror the differences in apparent molecular mass among oligomers filtrated and retained by 50 kDa cutoff membrane.

The same ATR-FTIR analyses were performed on the Aß42 peptide solubilized by protocol # 3, immediately after solubilization (Figure 5). This sample is characterized by the lowest amount of ß-sheet structures (Figure 5a) and 5c)) and by the highest ß-index value (Figure 5b)) as compared to the Aß42 peptides solubilized by protocol #1. We should note that the ~1695 cm^{-1} component is well resolved in the entire peptide and retained solution from protocol #1 while it is more overlapped with the near components in the filtrated solution from protocol #1 and in the entire peptide solution from protocol #3, leading to a possible overestimation of the ß-index value, markedly in the last case.

Since dehydration can affect the polypeptide secondary structures, particularly in the case of disordered proteins and peptides [49], we performed control experiments to compare the infrared response of Aß42 samples measured in form of a thin film (Figure 5 and Figure S6-) with that of Aß42 samples measured in solution (Figure S7). Very similar ATR-FTIR results were obtained with and without solvent evaporation for the entire peptide and retained solution from protocol #1. In the case of the filtrated sample from protocol #1 and of the entire peptide from protocol #3, the analyses of the ATR-FTIR spectra collected in solution indicate a lower content of ß-sheets and a higher α-helical/random coil structures (Figure S7), compared to secondary structures of the same Aß42 samples measured as a peptide film (Figure 5, Figure S6). In particular, the content of ß-sheet structures of the different Aß42 samples measured in solution was found to decrease in the following order (Figure S7-FTIR2): protocol #1, retained (65.10% ± 3.31); protocol #1, 2.5h (61.39% ± 4.53); protocol #1, filtrated (40.32% ± 8.03); protocol #3, t0 (26.96% ± 5.69). These data are consistent with ultrafiltration results (Figure 4d)). Altogether, the ATR-FTIR analyses of the different Aß42 samples measured as a thin peptide film or in solution consistently indicate a progressive increase of the ß-

sheet structures in the conversion of smaller species into larger assemblies, in agreement with what expected from their size.

3.3 Toxicity studies

The possibility to isolate aggregates by ultrafiltration also allows to consider these oligomeric populations as independent targets in toxicity tests, i.e. to verify whether aggregates of different size are endowed with different toxicity.

In vitro and *ex-vivo* toxicity of different Aß42 oligomers is controversial [9, 35, 36]; moreover, in this respect the supplier-to supplier variability of the synthetic Aß42 peptide is not addressed by the literature.

First, the ability of Aß42 *in toto* of inducing cell death on SH-SY5Y neuroblastoma cells was verified. For these experiments, cells were exposed to Aß42 (solubilized by following sample preparation protocol #3) after 10 days from solubilization, when both small and large oligomers are present. Compared to the control, 10 µM Aß42 induced a significant loss of cell viability (average ± SD : 79.44% ± 4.12, Figure 6). In the same fashion, toxicity experiments were independently carried out on oligomers filtrated and retained by a 50 kDa membrane (see Figure 4b) as explicative electrophoretic profiles). It is evident that monomers and dimers (peak 1 and 2) do not affect cell viability. Conversely, oligomers bigger than dodecamers (peak 3 in the electrophoretic pattern) are responsible for the toxicity of the entire Aß42 peptide, since they induce a cell death to an extent similar to that induced by the peptide *in toto* (cell viability, average ± SD : 80.09% ± 1.82).

4. CONCLUSIONS

Notwithstanding decades of research, the relationship between size, structure and toxicity of Aß42 oligomers remains unclear, also because of the difficulties in setting-up *in vitro* methods, to study the dynamic formation of such oligomers, to characterize the observed species and to independently assign toxicity. Since our pioneering work [21, 26-28], a few attempts have been made to describe Aß42 oligomerization *in vitro* by using CE as the main tool. CE separations published so far are almost exclusively confined to two main oligomeric populations that are rapidly precipitating and for which a dynamic equilibrium is often not demonstrated. These difficulties are unavoidably associated to poor peak area accuracy and reproducibility and make the applications of the methods intrinsically limited.

Here we have instead presented, over a wide time window, standardized and very reproducible analyses of soluble oligomeric populations that show multiple equilibria. When prepared by three different protocols, different aggregation dynamics of Aß42 peptide is clearly appreciated and accurately described. By a simple injection in CE we have also shown that a given sample preparation protocol may not be applicable to synthetic Aß42 peptides from different suppliers.

Conversely to what previously found by us, by ultrafiltration experiments followed by CE analyses monomers and dimers are detected using a less aggregating sample preparation (protocol #3), whereas by a more aggregating protocol (protocol #1), trimers represent the smallest specie formed. This finding is in contrast with what obtained by SDS-PAGE Western Blot, as it is highly possible that the formation of dimeric forms of Aß42 is an artefact of SDS-induced disaggregation [14, 46].

CE gives immediate access to semi-quantitative data on the proteinaceous material present in solution, on the dynamic formation of soluble oligomeric assemblies over time and on the reproducibility of the process. This means that CE preserves the native state of aggregates and should play a primary role in this kind of studies on aggregating peptides. The isolation of the separated species unequivocally identifies the absence of toxicity of oligomers with an apparent molecular mass lower than 50 kDa, namely equal or smaller than dodecamers, in particular monomers and dimers.

For the first time Aß42 oligomers isolated from a solution where they are at dynamic equilibrium are subjected to ATR-FTIR investigations through measurements both as a peptide film and in solution. Interestingly, the differences found in secondary structures are in agreement with the different oligomeric size distribution of the aggregates, as assessed by ultrafiltration. Indeed, α-helical/random coil structures are most abundant in smaller species, whereas a higher ß-sheet content characterizes the bigger and more toxic Aβ42 assemblies.

The integrative use of TEM, ATR-FTIR and cell-based assays clarifies and corroborates the results of the CE analysis. For all these reasons this approach is now adequate and complete enough to identify potential anti-oligomerization molecules and may help screening campaigns in drug discovery for Alzheimer's disease.

5. ACKNOWLEDGEMENTS

This work was supported by the University of Pavia (PhD student grant to FB); and by the University of Milano-Bicocca (research grant Fondo di Ateneo per la Ricerca to AN).

6. REFERENCES

[1] B. Winblad, P. Amouyel, S. Andrieu, C. Ballard, C. Brayne, H. Brodaty, A. Cedazo-Minguez, B. Dubois, D. Edvardsson, H. Feldman, L. Fratiglioni, G.B. Frisoni, S. Gauthier, J. Georges, C. Graff, K. Iqbal, F. Jessen, G. Johansson, L. Jonsson, M. Kivipelto, M. Knapp, F. Mangialasche, R. Melis, A. Nordberg, M.O. Rikkert, C. Qiu, T.P. Sakmar, P. Scheltens, L.S. Schneider, R. Sperling, L.O. Tjernberg, G. Waldemar, A. Wimo, H. Zetterberg, Defeating Alzheimer's disease and other dementias: a priority for European science and society, Lancet Neurol, 15 (2016) 455-532.

[2] S. Da Mesquita, A.C. Ferreira, J.C. Sousa, M. Correia-Neves, N. Sousa, F. Marques, Insights on the pathophysiology of Alzheimer's disease: The crosstalk between amyloid pathology, neuroinflammation and the peripheral immune system, Neurosci Biobehav Rev, 68 (2016) 547-562.

[3] S.J. Lee, E. Nam, H.J. Lee, M.G. Savelieff, M.H. Lim, Towards an understanding of amyloid-beta oligomers: characterization, toxicity mechanisms, and inhibitors, Chem Soc Rev, 46 (2017) 310-323.

[4] H.W. Querfurth, F.M. LaFerla, Alzheimer's disease, N Engl J Med, 362 (2010) 329-344.

[5] F. Chiti, C.M. Dobson, Protein Misfolding, Amyloid Formation, and Human Disease: A Summary of Progress Over the Last Decade, Annu Rev Biochem, 86 (2017) 35.1-35.42.

[6] A. Jan, O. Adolfsson, I. Allaman, A.L. Buccarello, P.J. Magistretti, A. Pfeifer, A. Muhs, H.A. Lashuel, Abeta42 neurotoxicity is mediated by ongoing nucleated polymerization process rather than by discrete Abeta42 species, J Biol Chem, 286 (2011) 8585-8596.

[7] J.A. Hardy, G.A. Higgins, Alzheimer's disease: the amyloid cascade hypothesis, Science, 256 (1992) 184-185.

[8] G. Bitan, M.D. Kirkitadze, A. Lomakin, S.S. Vollers, G.B. Benedek, D.B. Teplow, Amyloid beta -protein (Abeta) assembly: Abeta 40 and Abeta 42 oligomerize through distinct pathways, Proc Natl Acad Sci U S A, 100 (2003) 330-335.

[9] I. Benilova, E. Karran, B. De Strooper, The toxic Abeta oligomer and Alzheimer's disease: an emperor in need of clothes, Nat Neurosci, 15 (2012) 349-357.

[10] D.M. Walsh, D.J. Selkoe, A beta oligomers - a decade of discovery, J Neurochem, 101 (2007) 1172-1184.

[11] A. Jan, D.M. Hartley, H.A. Lashuel, Preparation and characterization of toxic Abeta aggregates for structural and functional studies in Alzheimer's disease research, Nat Protoc, 5 (2010) 1186-1209.

[12] W.B. Stine, L. Jungbauer, C. Yu, M.J. LaDu, Preparing synthetic Abeta in different aggregation states, Methods Mol Biol, 670 (2011) 13-32.

[13] M.Y. Suvorina, O.M. Selivanova, E.I. Grigorashvili, A.D. Nikulin, V.V. Marchenkov, A.K. Surin, O.V. Galzitskaya, Studies of Polymorphism of Amyloid-beta42 Peptide from Different Suppliers, J Alzheimers Dis, 47 (2015) 583-593.

[14] J.M. Mc Donald, G.M. Savva, C. Brayne, A.T. Welzel, G. Forster, G.M. Shankar, D.J. Selkoe, P.G. Ince, D.M. Walsh, The presence of sodium dodecyl sulphate-stable Abeta dimers is strongly associated with Alzheimer-type dementia, Brain, 133 (2010) 1328-1341.

[15] M.R. Nichols, B.A. Colvin, E.A. Hood, G.S. Paranjape, D.C. Osborn, S.E. Terrill-Usery, Biophysical comparison of soluble amyloid-beta(1-42) protofibrils, oligomers, and protofilaments, Biochemistry, 54 (2015) 2193-2204.

[16] D.C. Rambaldi, A. Zattoni, P. Reschiglian, R. Colombo, E. De Lorenzi, In vitro amyloid Abeta(1-42) peptide aggregation monitoring by asymmetrical flow field-flow fractionation with multi-angle light scattering detection, Anal Bioanal Chem, 394 (2009) 2145-2149.

[17] S.L. Bernstein, N.F. Dupuis, N.D. Lazo, T. Wyttenbach, M.M. Condron, G. Bitan, D.B. Teplow, J.E. Shea, B.T. Ruotolo, C.V. Robinson, M.T. Bowers, Amyloid-beta protein oligomerization and the importance of tetramers and dodecamers in the aetiology of Alzheimer's disease, Nat Chem, 1 (2009) 326-331.

[18] A. Abelein, J.D. Kaspersen, S.B. Nielsen, G.V. Jensen, G. Christiansen, J.S. Pedersen, J. Danielsson, D.E. Otzen, A. Graslund, Formation of dynamic soluble surfactant-induced amyloid beta peptide aggregation intermediates, J Biol Chem, 288 (2013) 23518-23528.

[19] S. Matsumura, K. Shinoda, M. Yamada, S. Yokojima, M. Inoue, T. Ohnishi, T. Shimada, K. Kikuchi, D. Masui, S. Hashimoto, M. Sato, A. Ito, M. Akioka, S. Takagi, Y. Nakamura, K. Nemoto, Y. Hasegawa, H. Takamoto, H. Inoue, S. Nakamura, Y. Nabeshima, D.B. Teplow, M. Kinjo, M. Hoshi, Two distinct amyloid beta-protein (Abeta) assembly pathways leading to oligomers and fibrils identified by combined fluorescence correlation spectroscopy, morphology, and toxicity analyses, J Biol Chem, 286 (2011) 11555-11562.

[20] M. Bartolini, M. Naldi, J. Fiori, F. Valle, F. Biscarini, D.V. Nicolau, V. Andrisano, Kinetic characterization of amyloid-beta 1-42 aggregation with a multimethodological approach, Anal Biochem, 414 (2011) 215-225.

[21] S. Sabella, M. Quaglia, C. Lanni, M. Racchi, S. Govoni, G. Caccialanza, A. Calligaro, V. Bellotti, E. De Lorenzi, Capillary electrophoresis studies on the aggregation process of beta-amyloid 1-42 and 1-40 peptides, Electrophoresis, 25 (2004) 3186-3194.

[22] D. Brinet, J. Kaffy, F. Oukacine, S. Glumm, S. Ongeri, M. Taverna, An improved capillary electrophoresis method for in vitro monitoring of the challenging early steps of Abeta1-42 peptide oligomerization: application to anti-Alzheimer's drug discovery, Electrophoresis, 35 (2014) 3302-3309.

[23] D. Brinet, F. Gaie-Levrel, V. Delatour, J. Kaffy, S. Ongeri, M. Taverna, In vitro monitoring of amyloid beta-peptide oligomerization by Electrospray differential mobility analysis: An alternative tool to evaluate Alzheimer's disease drug candidates, Talanta, 165 (2017) 84-91.

[24] R. Picou, J.P. Moses, A.D. Wellman, I. Kheterpal, S.D. Gilman, Analysis of monomeric Abeta (1-40) peptide by capillary electrophoresis, Analyst, 135 (2010) 1631-1635.

[25] R.A. Picou, I. Kheterpal, A.D. Wellman, M. Minnamreddy, G. Ku, S.D. Gilman, Analysis of Abeta (1-40) and Abeta (1-42) monomer and fibrils by capillary electrophoresis, J Chromatogr B Analyt Technol Biomed Life Sci, 879 (2011) 627-632.

[26] R. Colombo, A. Carotti, M. Catto, M. Racchi, C. Lanni, L. Verga, G. Caccialanza, E. De Lorenzi, CE can identify small molecules that selectively target soluble oligomers of amyloid beta protein and display antifibrillogenic activity, Electrophoresis, 30 (2009) 1418-1429.

[27] S. Butini, M. Brindisi, S. Brogi, S. Maramai, E. Guarino, A. Panico, A. Saxena, V. Chauhan, R. Colombo, L. Verga, E. De Lorenzi, M. Bartolini, V. Andrisano, E. Novellino, G. Campiani, S. Gemma, Multifunctional cholinesterase and amyloid Beta fibrillization modulators. Synthesis and biological investigation, ACS Med Chem Lett, 4 (2013) 1178-1182.

[28] S. Brogi, S. Butini, S. Maramai, R. Colombo, L. Verga, C. Lanni, E. De Lorenzi, S. Lamponi, M. Andreassi, M. Bartolini, V. Andrisano, E. Novellino, G. Campiani, M. Brindisi, S. Gemma, Disease-modifying anti-Alzheimer's drugs: inhibitors of human cholinesterases interfering with beta-amyloid aggregation, CNS Neurosci Ther, 20 (2014) 624-632.

[29] M. Bartolini, C. Bertucci, M.L. Bolognesi, A. Cavalli, C. Melchiorre, V. Andrisano, Insight into the kinetic of amyloid beta (1-42) peptide self-aggregation: elucidation of inhibitors' mechanism of action, Chembiochem, 8 (2007) 2152-2161.

[30] M.T. Ackermans, F.M. Everaerts, J.L. Beckers, Quantitative analysis in capillary zone electrophoresis with conductivity an indirect UV detection, J Chrom A, 549 (1991) 345-355.

[31] E. Cerf, R. Sarroukh, S. Tamamizu-Kato, L. Breydo, S. Derclaye, Y.F. Dufrene, V. Narayanaswami, E. Goormaghtigh, J.M. Ruysschaert, V. Raussens, Antiparallel beta-sheet: a signature structure of the oligomeric amyloid beta-peptide, Biochem J, 421 (2009) 415-423.

[32] R. Sarroukh, E. Goormaghtigh, J.M. Ruysschaert, V. Raussens, ATR-FTIR: a "rejuvenated" tool to investigate amyloid proteins, Biochim Biophys Acta, 1828 (2013) 2328-2338.

[33] A. Natalello, S.M. Doglia, Insoluble protein assemblies characterized by fourier transform infrared spectroscopy, Methods Mol Biol, 1258 (2015) 347-369.

[34] A. Natalello, P.P. Mangione, S. Giorgetti, R. Porcari, L. Marchese, I. Zorzoli, A. Relini, D. Ami, G. Faravelli, M. Valli, M. Stoppini, S.M. Doglia, V. Bellotti, S. Raimondi, Co-fibrillogenesis of Wild-type and D76N beta2-Microglobulin: the crucial role of fibrillar seeds, J Biol Chem, 291 (2016) 9678-9689.

[35] G.M. Shankar, S. Li, T.H. Mehta, A. Garcia-Munoz, N.E. Shepardson, I. Smith, F.M. Brett, M.A. Farrell, M.J. Rowan, C.A. Lemere, C.M. Regan, D.M. Walsh, B.L. Sabatini, D.J. Selkoe, Amyloid-beta protein dimers isolated directly from Alzheimer's brains impair synaptic plasticity and memory, Nat Med, 14 (2008) 837-842.

[36] S. Lesne, M.T. Koh, L. Kotilinek, R. Kayed, C.G. Glabe, A. Yang, M. Gallagher, K.H. Ashe, A specific amyloid-beta protein assembly in the brain impairs memory, Nature, 440 (2006) 352-357.

[37] W.B. Stine, Jr., K.N. Dahlgren, G.A. Krafft, M.J. LaDu, In vitro characterization of conditions for amyloid-beta peptide oligomerization and fibrillogenesis, J Biol Chem 278 (2003) 11612-11622.

[38] D. Thirumalai, G. Reddy, J.E. Straub, Role of water in protein aggregation and amyloid polymorphism, Acc Chem Res, 45 (2012) 83-92.

[39] K. Klement, K. Wieligmann, J. Meinhardt, P. Hortschansky, W. Richter, M. Fandrich, Effect of different salt ions on the propensity of aggregation and on the structure of Alzheimer's abeta(1-40) amyloid fibrils, J Mol Biol, England, 373 (2007) 1321-1333.

[40] M. Garvey, K. Tepper, C. Haupt, U. Knupfer, K. Klement, J. Meinhardt, U. Horn, J. Balbach, M. Fandrich, Phosphate and HEPES buffers potently affect the fibrillation and oligomerization mechanism of Alzheimer's Abeta peptide, Biochem Biophys Res Commun, 409 (2011) 385-388.

[41] M. Kato, H. Kinoshita, M. Enokita, Y. Hori, T. Hashimoto, T. Iwatsubo, T. Toyo'oka, Analytical method for beta-amyloid fibrils using CE-laser induced fluorescence and its application to screening for inhibitors of beta-amyloid protein aggregation, Anal Chem, 79 (2007) 4887-4891.

[42] F. Yin, J. Liu, X. Ji, Y. Wang, J. Zidichouski, J. Zhang, Silibinin: a novel inhibitor of Abeta aggregation, Neurochem Int, 58 (2011) 399-403.

[43] C.L. Shen, R.M. Murphy, Solvent effects on self-assembly of beta-amyloid peptide, Biophys J, 69 (1995) 640-651.

[44] K. Broersen, W. Jonckheere, J. Rozenski, A. Vandersteen, K. Pauwels, A. Pastore, F. Rousseau, J. Schymkowitz, A standardized and biocompatible preparation of aggregate-free amyloid beta peptide for biophysical and biological studies of Alzheimer's disease, Protein Eng Des Sel, 24 (2011) 743-750.

[45] M. Quaglia, E. De Lorenzi, Capillary electrophoresis in drug discovery, Methods Mol Biol, 572 (2009) 189-202.

[46] A.D. Watt, K.A. Perez, A. Rembach, N.A. Sherrat, L.W. Hung, T. Johanssen, C.A. McLean, W.M. Kok, C.A. Hutton, M. Fodero-Tavoletti, C.L. Masters, V.L. Villemagne, K.J. Barnham, Oligomers, fact or artefact? SDS-PAGE induces dimerization of beta-amyloid in human brain samples, Acta Neuropathol, 125 (2013) 549-564.

[47] A. Barth, Infrared spectroscopy of proteins, Biochim Biophys Acta, 1767 (2007) 1073-1101.

[48] M. Baldassarre, C.M. Baronio, L.A. Morozova-Roche, A. Barth, Amyloid β-peptides 1-40 and 1-42 form oligomers with mixed β-sheets, Chem Sci, 8 (2017) 8247-8254).

[49] A. Natalello, V.V. Prokorov, F. Tagliavini, M. Morbin, G. Forloni, M. Beeg, C. Manzoni, L. Colombo, M. Gobbi, M. Salmona, S.M. Doglia, Conformational plasticity of the Gerstmann-Straussler-Scheinker disease peptide as indicated by its multiple aggregation pathways, J Mol Biol, 381 (2008) 1349-1361.

FIGURE LEGENDS

Figure 1. Protocol #1. Oligomerization process of Aß42 monitored over time by CE (method A). a) Top: representative electrophoretic profiles of Aß42 (221 µM) at different elapsed times from t0 until sample precipitation and average effective electrophoretic mobilities (μ_{eff}) of detected peaks, (n=5 independent experiments). Insets: representative TEM images of amyloid fibrils at t0 and at sample precipitation, (n=3); scale bar: 100 nm. Bottom: average, SD and relative standard deviation (RSD) of μ_{eff} of detected peaks. **b)** Plot of the normalized peak area % at different elapsed times of peak A, peak B and peak C, during the first 30 hours, when dynamic equilibrium is evident. Each monitoring point is in triplicate, error bars correspond to SD.

Figure 2. Protocol #2. Oligomerization process of Aß42 monitored over time by CE (method A, redissolution in 100% DMSO). Monitoring of Aß42 (221 µM) aggregation process from t0 up to 28 days, CE traces are representative of n=3 independent experiments. The off-scale EOF signal is truncated for clarity. Inset: representative TEM image of amorphous aggregates observed at t0 and at sample precipitation; scale bar: 100 nm.

Figure 3. Protocol #3. Oligomerization process of Aß42 monitored over time by CE (method B). a) Top: representative electrophoretic profiles of Aß42 (100 µM) at different elapsed times from t0 until the end of aggregation process, (n=5 independent experiments). Inset: amyloid fibrils identified by TEM analysis at t0 and at sample precipitation; scale bar: 100 nm. Bottom: average, SD and RSD of μ_{eff} of detected peaks. b) Plot of the normalized peak area % over time of peak 1, peak 2 and peak 3. Each monitoring point is in triplicate, error bars correspond to SD.

Figure 4. UF characterization of Aß42 oligomers. Ultrafiltration experiments with a) 100, b) 50, c) 30 and d) 10 kDa with Aß42 solubilized by following protocol #1 and protocol #3.

Figure 5. ATR-FTIR characterization of Aß42 oligomers. a) FSD spectra of different Aß42 preparations showed in the Amide I band. b) The ß-index values (intensity ratio ~1695/~1630) calculated from the baseline corrected FSD spectra. c) Total content of the ß-sheet structures evaluated by curve-fitting analysis of the FSD spectra. The ATR-FTIR spectra were collected after solvent evaporation, corrected for the buffer absorption and normalized at the Amide I band area before FSD. The reported data refer to the average and standard deviation obtained from three independent Aß42 preparations. Analysed samples: Aß42 from protocol # 1 before ultrafiltration (Prot #1, 2.5h), retained (Prot #1 R, 2.5 h) and filtrated (Prot #1 F, 2.5 h) through a 50 kDa membrane; entire Aß42 peptide solubilized by protocol # 3 (Prot #3 t0).

Figure 6. MTT test. Entire Aß42 peptide and oligomers lower and bigger than 50 kDa (sample preparation protocol #3, 10 days). Data are expressed as cell viability of control, error bars represent SD (n=3).

AN INTEGRATED STRATEGY TO CORRELATE AGGREGATION STATE, STRUCTURE AND TOXICITY OF Aß 1-42 OLIGOMERS.

Federica Bisceglia [a], Antonino Natalello [b], Melania Maria Serafini [a,c], Raffaella Colombo [a], Laura Verga [d], Cristina Lanni [a], Ersilia De Lorenzi [a]

[a] Department of Drug Sciences, University of Pavia, Viale Taramelli 12, 27100, Pavia, Italy.

[b] Department of Biotechnology and Biosciences, University of Milano Bicocca, Piazza della Scienza 2, 20126, Milano, Italy.

[c] Scuola Universitaria Superiore IUSS Pavia, Piazza della Vittoria 15, 27100, Pavia, Italy.

[d] Unit of Pathology, IRCCS Policlinico S. Matteo Foundation and University of Pavia, Via Forlanini 14, 27100, Pavia, Italy.

Corresponding author:

Prof. Ersilia De Lorenzi,

Department of Drug Sciences, University of Pavia, v.le Taramelli 12, 27100, Pavia.

email: ersidelo@unipv.it

tel +39 0382 987747

fax +39 0382 422975

Keywords: Alzheimer's disease; Capillary electrophoresis; Aß 1-42; Aß oligomers; Sample preparation; Fourier transform infrared spectroscopy.

Abbreviations: Aß, Amyloid-beta; Aß42, Aß 1-42; CE, capillary electrophoresis; AD, Alzheimer's disease; TEM, transmission electron microscopy; ATR-FTIR, Attenuated total reflection-Fourier transform infrared; FSD, Fourier self deconvolution; EOF, electroosmotic flow.

ABSTRACT

Despite great efforts, it is not known which oligomeric population of amyloid beta (Aß) peptides is the main neurotoxic mediator in Alzheimer's disease. *In vitro* and *in vivo* experiments are challenging, mainly because of the high aggregation tendency of Aß (in particular of Aß 1-42 peptide), as well as because of the dynamic and non covalent nature of the prefibrillar aggregates. As a step forward in these studies, an analytical platform is here proposed for the identification and characterization of Aß 1-42 oligomeric populations resulting from three different sample preparation protocols. To preserve the transient nature of aggregates, capillary electrophoresis is employed for monitoring the oligomerization process in solution until fibril precipitation, which is probed by transmission electron microscopy. Based on characterization studies by ultrafiltration and SDS-PAGE/Western Blot, we find that low molecular weight oligomers build up over time and form bigger aggregates (> dodecamers) and that the kinetics strongly depends on sample preparations. The use of phosphate buffer results to be more aggregating, since trimers are the smallest species found in solution, whereas monomers and dimers are obtained by solubilizing Aß 1-42 in a basic mixture. For the first time, attenuated total reflection-Fourier transform infrared spectroscopy is used to assign secondary structure to the separated oligomers. Random coil and/or α-helix are most abundant in smaller species, whereas ß-sheet is the predominant conformation in bigger aggregates, which in turn are demonstrated to be responsible for Aß 1-42 toxicity.

1. INTRODUCTION

It is estimated that more than 30 million people worldwide suffer from Alzheimer's disease (AD) [1]. The evidence that different molecular pathways are involved in neurodegeneration makes AD a multifactorial disease [2] and this explains the difficulties in defining the aetiology and in discovering effective treatments [1, 3]. Among many factors, it is now well established that the soluble aggregates of amyloid-beta (Aß) protein play a crucial role in the onset of the disease and therefore studying their self-assembly is the focus of intense research. Aß protein is a family of peptides that ranges from 36 to 43 amino acids and derives from the proteolytic cleavage of the amyloid precursor protein (APP) [4]. Unfolded or partially folded Aß monomers interact through a nucleation-elongation process to form small oligomers and nuclei that rapidly lead to larger aggregates and then to fibrillar forms [5, 6]. In turn, the insoluble amyloid fibrils deposit in the brain as extracellular amyloid plaques which represent one of the two hallmarks of AD, together with neurotangles of hyperphosphorylated tau protein [1, 5]. In the last two decades the soluble pre-fibrillar oligomers of Aß peptides have been recognised as the principal neurotoxic mediators which lead to detrimental effects on the AD brain [3, 7, 8]. Despite significant efforts, the structure of these Aß oligomers, the understanding at the molecular level of their aggregation process, the exact mechanism of oligomer-induced toxicity as well as the accurate identification of the neurotoxic oligomeric species, remain elusive. Intrinsic limitations in investigating Aß oligomers are mainly related to their peculiar nature: they consist of heterogeneous populations of polymorphic, non-covalent and transiently populated aggregates generated by multiple pathways. This is true especially for Aß 1-42 (Aß42), which is the most amyloidogenic and toxic among the Aß peptides [3, 8, 9].

Important progress has been made through *ex vivo* and *in vitro* studies performed either with AD brain-derived oligomers or synthetic peptides. Because of the target organ of amyloid aggregates, the availability of brain-derived species is clearly restricted and *ex vivo* studies are difficult to approach [9, 10]. In principle, by using synthetic peptides a strict control of the starting material and a modulation of the aggregation process could be achieved, even if exact physiological conditions cannot be replicated. On the other hand, because of their high aggregation tendency, and in particular that of Aß42, a fine tuning of the oligomer formation and kinetics is challenging. Each specific solubilization protocol (different solvents, peptide concentrations, incubation time and temperature) leads to different oligomeric species [11, 12]. Notably, authors very often claim the presence in solution of aggregates of defined size on the basis of previous literature data that report the same or similar sample preparation. In this specific context it is easy to make wrong assumptions, also because synthetic peptides are characterized by extreme variability including supplier-to-supplier and batch-to-batch, an issue that is rarely addressed [13]. These limitations, together with the complex dynamic equilibrium existing among Aß species contribute to the widespread and controversial literature on Aß oligomers [3, 9].

Complementary information on the isolation and size estimation of Aß aggregates and the related toxicity has been achieved over the years by multiple techniques such as SDS-PAGE [8, 14] size exclusion chromatography (SEC) [15], dynamic and multiangle light scattering (DLS and MALS) [15, 16], microscopy [5], mass spectrometry [17], NMR spectroscopy and X-ray crystallography [18]. Each technique is not devoid of limitations and drawbacks. These are mainly related to the non covalent and dynamic nature of Aß oligomers and to the ability of a technique to provide information on small and large oligomers with an equivalent accuracy. For example, DLS and MALS can not intrinsically separate different oligomeric populations for independent characterization [3, 10]; fluorescence-based detectors require non-native labelled peptides that may alter the oligomerization kinetics [19]; both MALDI and ESI ionization sources may induce oligomer dissociation[20]. Some authors successfully stabilized the transient nature of oligomers by photo-induced cross-linking, to analyze the resulting "frozen" oligomers by SEC or SDS-PAGE [8]. While this procedure overcomes the dissociation induced by e.g. SDS-PAGE, it also implies that oligomers do not exactly mirror the native state in solution.

The use of capillary electrophoresis (CE) with UV detection to monitor *in vitro* Aß oligomer formation was pioneered by our group [21]. CE works in free solution and in the absence of a stationary phase or chaotropic agents, thus it preserves the native oligomeric structure and provides a real time snapshot of different soluble and unlabelled Aß assemblies during their formation.

Over the years CE-UV was employed to detect and separate soluble oligomeric species of Aß peptides ranging from monomers [22-25] to aggregates larger than dodecamers [21, 22, 26-28]. To provide oligomer size characterization, CE separation was also used concurrently with Taylor dispersion analysis [22], ultrafiltration [21, 26-28], MALDI-TOF [25] and very recently electrospray differential mobility analysis [23]. In these works the CE separation is limited to two main oligomeric populations that are rapidly precipitating and for which a dynamic equilibrium is often not demonstrated. Here instead we initially focus on the effect that different Aß42 sample preparation protocols have on the formation of assemblies in solution; experimental conditions are finely tuned so to obtain and separate by CE as many oligomeric populations as possible and to considerably extend the time window over which these oligomers are soluble. Not only does this approach enable an easier isolation of the separated species by ultrafiltration and the assignment of their cell toxicity, but also it makes possible for the first time an independent analysis of their secondary structure by attenuated total reflection-Fourier transform infrared (ATR-FTIR) spectroscopy. Finally, it is shown how a simple CE analysis of Aß42 can shed light on a crucial issue whose importance is hardly ever addressed: peptide batch-to-batch and supplier-to-supplier reproducibility.

2. MATERIALS AND METHODS

2.1 Materials

Synthetic Aß42 (MW 4514.10 Da) was purchased as lyophilized powder from Anaspec (Fremont, CA, USA), (purity ≥ 95%; lots #1556608, #1556609, #1457203) and Bachem (Bubendorf, Switzerland), (purity ≥ 95%; lots #10533163, #1065556, #1056654) and stored at -20°C. 1,1,1,3,3,3-Hexafluoropropan-2-ol (HFIP), dimethylsulfoxide (DMSO), acetonitrile (ACN), and sodium carbonate were from Sigma-Aldrich (St. Louis, MO, USA). Sodium hydroxide and sodium dodecyl sulphate (SDS) were provided by Merck (Darmstadt, Germany). Na_2HPO_4 and NaH_2PO_4, supplied by Sigma-Aldrich, were used for the preparation of the background electrolyte (BGE) in the CE analyses. BGE solutions were prepared daily using Millipore Direct-Q™ deionized water (Bedford, MA, USA) and filtered with 0.45 µm Sartorius membrane filters (Göttingen, Germany).

Ultrafiltration devices (10, 30 and 100 kDa cutoff) were purchased from Pall Corporation (New York, NY, USA), whereas 50 kDa cutoff membranes were from Millipore (Billerica, MA, USA).

The 3-(4,5-dimethylthiazol-2-yl)-2,5-diphenyl-tetrazolium bromide (MTT) and phosphate buffered saline (PBS) employed in the cell viability assay were supplied by Sigma-Aldrich.

2.2 Solubilization protocols

Aß42 oligomers were prepared by following three different solubilization protocols.

Protocol #1: Aß42 (Anaspec) was solubilized in HFIP (1 mg/mL, ~ 221 µM). The stock solution was gently mixed and then kept for 30 minutes at 4°C, aliquoted in microfuge tubes and lyophilized via Speed-Vac. Then Aß42 aliquots were redissolved in 20 mM Na_2HPO_4/NaH_2PO_4, pH 7.4.

Protocol #2: Aß42 (Anaspec) aliquots were prepared as in #1 and then redissolved in DMSO/20 mM phosphate buffer (pH 7.4) at increasing concentrations of DMSO.

Protocol #3: Aß42 (Bachem) was prepared as described by Bartolini *et al* [29]. Briefly, the peptide was solubilized in HFIP (149 µM) and kept at room temperature overnight. The stock solution was aliquoted in microfuge tubes and kept at room temperature for one day, then HFIP was left to evaporate overnight. The resulting peptide film was redissolved to obtain 500 µM Aß42: the redissolution mixture consisted of ACN/300 µM Na_2CO_3/250 mM NaOH (48.3:48.3:3.4, v/v/v). The final peptide solution (100 µM) was obtained by the dilution of 500 µM Aß42 with 20mM Na_2HPO_4/NaH_2PO_4 (pH=7.4).

For all protocols final solutions were not centrifuged, to avoid mechanical stress at the beginning of the aggregation process.

2.3 Capillary electrophoresis and ultrafiltration

Aß42 samples were analyzed by CE at different elapsed times from t0, where t0 is defined as the time when the HFIP-lyofilized peptide is redissolved.

CE analyses were performed on an Agilent Technologies 3D CE system (Waldbronn, Germany) equipped with a diode-array detector (DAD) set at λ=200 nm. Data were collected using Chemstation A.10.02 software.

In the present work, two CE methods (A and B) were applied. Uncoated fused-silica capillaries provided by Polymicro Technologies (Phoenix, AZ, USA) were pretreated by flushing 1 M NaOH, deionized water and BGE (80 mM sodium phosphate buffer, pH=7.4) for 60 min, 60 min and 90 min (method A), or for 30 min, 30 min and 60 min (method B), respectively. BGE was prepared by mixing 80 mM solutions of Na_2HPO_4 and NaH_2PO_4 in order to obtain the desired pH.

In method A [28] the analytical separation was carried out at 16 kV (current: 75-80 μA) on a capillary of 53 cm of total length (L=53 cm, l=44.5 cm). Samples were hydrodynamically injected by applying 50 mbar for 8 s. In method B, a capillary of L=33 cm, l= 24.5 cm was used; the applied voltage was 12 kV (current 75-80 μA) and hydrodynamic injection parameters were set at 30 mbar for 3 s. For both methods the capillary temperature was 25°C and the between-run rinsing cycle consisted of 50 mM SDS (1.5 min), deionized water (1.5 min), and BGE (2 min).

The electroosmotic flow (EOF) is easily measured as a perturbation of the baseline given by solvents used for the redissolution of the lyophylized Aß42 aliquots and thus it is considered as a reliable noninteracting marker. The effective mobilities (μ_{eff}, $cm^2V^{-1}s^{-1}$) of each peak are calculated by subtracting the contribute of the EOF (μ_{EOF}) from the apparent mobility (μ_{app}, $cm^2V^{-1}s^{-1}$). Semiquantitative analyses were performed based on the normalized area % [30]. Aß42 peptide solutions were ultrafiltrated on devices at different elapsed times from t0 and the resulting filtrated and retained solutions were analyzed by CE. Ultrafiltration experiments were carried out in triplicate and by applying the best experimental conditions for each type of membrane, as suggested by suppliers: 14000 g for 10 minutes with 10, 30, and 100 kDa cutoff membranes and 60 minutes with 50 kDa cutoff membranes. In order to obtain enough volume of the retained solutions and to approximately restore the original concentration, a volume of 20 mM phosphate buffer (pH 7.4), equal to that of the ultrafiltrated sample, was added to the retained portion that was recovered by reverse spinning (14000 g, 5 minutes, for 50 kDa membrane). For 10, 30 and 100 kDa devices, since the reverse spinning is not intrinsically possible because of their geometry, the retained portion was recovered by using a micropipette.

Appropriate quantification of the retained sample amount is clearly not possible. However, the comparison of the electropherograms obtained before and after ultrafiltration was used to verify that the concentrations of the injected species were qualitatively comparable.

2.4 Transmission electron microscopy

Precipitated samples were fixed on carbon-coated Formvar nickel grids (200 mesh) (Electron Microscopy Sciences, Washington, PA, USA). Aß42 suspensions were diluted to 10 µM with 20 mM phosphate buffer (pH 7.4). Ten µL suspension were left to sediment on grids; after 15 minutes the excess of sample was drained off by means of a filter paper. The negative staining was performed with 10 µL of 2% w/v uranyl acetate solution (Electron Microscopy Sciences). Sample investigations were carried out in triplicate by using a JEOL JEM 1400-Plus electron microscope, operating at 80 kV (Peabody, MA, USA).

2.5 Fourier Transform Infrared spectroscopy

Structural properties of Aß42 solubilized by protocol #1 and protocol #3 and those of filtrated and retained solutions on 50 kDa cutoff membrane were analyzed by FTIR measurements in attenuated total reflection (ATR) [31-34]. For these analyses, 2 µl of each sample were deposed on the single reflection diamond crystal of the ATR device (Quest ATR, Specac, Orpington, UK). In order to obtain a hydrated peptide film, samples were dried [31] at room temperature.The ATR-FTIR spectra of the hydrated films were recorded by a Varian 670-IR spectrometer (Varian Australia Pty Ltd, Mulgrave VIC, Australia), which was continuously purged with dried air. Conditions applied were: 2 cm^{-1} resolution, scan speed of 25 kHz, 1000 scan coadditions, triangular apodization, and a nitrogen-cooled Mercury Cadmium Telluride detector [34]. The measured spectra were normalized at the area of the Amide I band (around 1700-1600 cm^{-1}) to compensate for possible differences in the peptide content. Fourier self deconvolution (FSD) was obtained with a full width at half height of 13.33 cm^{-1} and a resolution enhancement factor K = 1.5. Spectral collection, the FSD and the second derivative analyses [33] were performed using the Resolutions-Pro software (Varian Australia Pty Ltd). The evaluation of the peptide secondary structures was obtained by curve-fitting of the FSD spectra in the Amide I spectral region [31, 33]. Because the result of this procedure is not unique, the selection of the input parameter is very important. Here a linear baseline was employed and the number and peak position of the initial components were taken from the second derivative and FSD spectra. Curve-fitting was performed by leaving the initial parameters (baseline, peak position, band width, and band intensity) free to adjust iteratively with the only exception of the two Amide I components assigned to β-sheet structures (around 1633-1628 cm^{-1} and around 1695-1692 cm^{-1}, respectively [31, 33]), whose positions were restricted within 4 cm^{-1} from the wavenumbers observed in the second derivative spectra. The same set of input parameters were employed for the curve-fitting of the FSD spectra of the different Aß42 preparations, to allow a more reliable evaluation of the differences in the secondary structure content among the analyzed samples. The curve-fitting was performed using the GRAMS/AI 8.0 software (Thermo Electron Corporation, Waltham, USA).

In control experiments, the same Aβ42 preparations were measured in ATR without solvent evaporation [33]. For these analyses, 20 µl of each sample were deposed on the nine-reflection diamond crystal of the ATR device (DuraSamplIR II, Smith Detection, USA) and the ATR-FTIR spectra were immediately collected as described above. The peptide spectra were obtained after subtraction of the buffer contribution and analysed following the same procedures employed for the peptide film spectra.

2.6 SH-5YSY cell viability assay

SH-SY5Y human neuroblastoma cell cultures (ECACC No. 94030304) were grown at 37°C in 5% CO_2/95% air in a medium composed of Eagle's minimum essential medium and Nutrient Mixture Ham's F-12, with the addition of 10% FBS, 2 mM glutamine, penicillin/streptomycin, non essential amino acids. All culture media and supplements were purchased from Euroclone (Life Science Division, Milan, Italy).

The MTT colorimetric assay based on the reduction of MTT by mitochondrial dehydrogenase was employed to evaluate the cellular redox activity as initial indicator of cell death. At day 0, SH-SY5Y cells were plated at a density of $5x10^4$ viable cells *per* well in 96-well plates. The next day, cells were exposed to approximately 10 µM entire Aß42 peptide (prepared according to protocol #3) for 24 h at 37°C or to filtrated and retained solutions obtained after ultrafiltration experiments and then to a MTT solution in PBS (1 mg/mL). After 4 h incubation, cells were lysed with lysis buffer (20% SDS in water/dimethylformamide 1:1) and incubated overnight at 37°C. The cell viability reduction was quantified by using a Sinergy HT microplate reader (Biotek, Winooski, Vermont, USA).

For statistical analysis the GraphPad Instat statistical package (version 3.05 GraphPad software, San Diego, CA, USA) was used. Data were analyzed by analysis of variance (ANOVA) followed, if significant, by an appropriate post hoc comparison test. The reported data are expressed as mean ± standard deviation (SD) of three independent experiments. Values of $p<0.05$ were considered statistically significant.

3. RESULTS AND DISCUSSION

3.1 Monitoring of Aß42 aggregation process by CE

Both small and large oligomers seem to exert neurotoxicity and also the ongoing polymerization process may be responsible for Aß toxicity and neurodegeneration in AD [6, 9].

Over the years increasing attention has been paid towards small oligomers deemed to be toxic such as monomers, dimers, trimers, tetramers, nonamers and dodecamers [14, 17, 35, 36].

Therefore, aim of this work is also to promote the formation of low MW species and to demonstrate the existing dynamic equilibrium by keeping the formed assemblies soluble for a wide time window. In this way we intend to overcome the limitations very often shown by existing CE-based experiments: data obtained on short-lived (i.e. rapidly precipitating) samples, separation of two main oligomeric populations only [23, 25, 28], lack of properly replicated data over a defined time frame, little or no characterization of the separated species and of the final precipitates.

The outline of the sample preparation protocols is reported in Figure S1. The three procedures share an initial treatment with HFIP then, depending on the degree of aggregation required, different solvents have been employed. As demonstrated by circular dichroism and atomic force microscopy data [29, 37], fluorinated alcohols like HFIP are able to promote α-helix conformation and disrupt ß-sheet structures, thus erasing the "structural history" of Aß42 [12].

Notably, in all experiments we kept the operative current value very similar to that reported in [21, 26] so as to ensure that the electric field does not influence the strength of the noncovalent intermolecular interactions that sustain the peptide oligomerization, as demonstrated in [21].

3.1.1 Protocol #1

The dried film obtained after lyophilization of the HFIP-solubilized peptide is redissolved in phosphate buffer at physiological pH, to trigger the formation of aggregates. In general, salts dissolved in aqueous solutions have an important role in promoting protein-protein association. Salts can reduce repulsive electrostatic interactions through an increase of the apparent dielectric constant of water and can interact with charged or polar residues thus stabilizing salt bridges [38, 39]. Because of specific interactions with Aß histidine residues, phosphate ions have been reported to strongly affect the fibrillogenesis and oligomerization of amyloid peptides [40].

Figure 1a) shows a selection of CE traces of the same peptide sample when injected at different elapsed times from t0. Electropherograms are representative of one out of five independent experiments. Conversely to what reported in previous work by us [21, 26-28] and sometimes by others [22, 41], this sample preparation affords detectable soluble species over a time window which is up to more than 10 folds longer, before precipitation. Given the very high aggregation tendency of Aß42, the likely presence of insoluble material in the solutions used in many experiments affects data reproducibility and accuracy and,

obviously, also aggregation kinetics and toxicity data. Declaration and demonstration of the time span over which the prepared sample is soluble is rarely found and nevertheless it is mandatory, if sound results have to be produced. In this respect, a technique that works in free solution such as CE is an asset, as the presence of in-capillary insoluble material, adhesion phenomena and unwanted interactions with the capillary wall are easily spotted by spikes in the electropherogram, current fluctuations or dropping, irreproducible migration times and peak areas.

In Figure 1a) three peaks are separated. Notably, the effective mobilities (μ_{eff} values) are averaged on 10 monitoring times from 5 independent experiments, using three different peptide batches from the same supplier (Anaspec). The excellent RSD% values allow peak labelling as A, B and C all the way through the monitoring time, on the basis of precise electrophoretic mobilities. Conversely to what reported by using different [21, 26-28] or similar [25] sample preparations, Figure 1a) reveals that, already immediately after redissolution of the dried film, the earlier migrating peak A is the most abundant and aggregation has already started, as two more peaks are present.

Transmission electron microscopy (TEM) image taken at t0 in Figure 1a), representative of three independent experiments, reveals that also fibrils are present in this sample: as the solution is neither stirred nor centrifuged before analysis, it is likely that they are sedimented at the bottom of the anodic vial and thus they are not injected into the capillary, as confirmed by the absence of spikes in the electropherogram. Since oligomers and fibrils are at equilibrium in the brain [9] this protocol better mimics *in vivo* conditions, as compared to protocols that force the apparent formation of monomers [22].

According to our previous work [21, 26-28], and following the hypothesis that mass prevails over charge in the migration observed, it is plausible to anticipate that the faster migrating population corresponds to low MW oligomers (peak A), whereas peaks B and C should be higher MW species. Bearing in mind this hypothesis and as a preliminary investigation, four solutions injected in CE (at t0, 5.5 h, 81 h and 5 days) have been analyzed by SDS-PAGE/Western Blot (Figure S2). Bands ranging from dimers up to 22-mers are detected. Contrary to CE data, bands relative to large oligomers are observed in WB analyses only at a late stage of the aggregation process. Further, bands corresponding to Aß42 dimers up to tetramers are abundant even at 81 h and 5 days, when the electrophoretic peak A has already totally converted into larger aggregates.

Because standards are not available, a quantitative evaluation of the oligomers observed in CE is intrinsically unaccessible. Notwithstanding this limitation, a CE semi-quantitative analysis based on normalized peak area percent [30] is carried out in triplicate: for each monitoring point, SD is lower than 9%. In Figure S3a) (Supplementary material), the normalized areas over the entire time span are provided, and in Figure 1b), a focus on the early aggregation times up to 72 hours can be found. Altogether, it is clear that with the progression of the self-assembly process, the putative small oligomers (peak A) are depleted and contribute to the formation of peaks B and C, possibly corresponding to larger species. At later times

only peak C is detected. More in detail, peaks B and C are at mutual equilibrium within the first 72 hours: the area of peak B increases and that of peak C decreases and vice versa. This could be well one of the several equilibria hypothesized among oligomers [3, 9], that is kept inside the capillary where species are free to interconvert. The observation of a sharp and efficient peak (peak C) after a broad band such as peak B, may suggest ongoing precipitation and the presence of a spike [22, 25, 41]. However, three pieces of evidence rule out this hypothesis: i) the dynamic equilibrium between peak B and peak C; ii) the high reproducibility of peak C mobility; iii) the UV spectrum taken by DAD detector, similar to that obtained for the other peaks relative to Aß peptide (Figure S3b)). At the end of the aggregation process no more peaks are detected by CE, the sample is visibly cloudy and the TEM analysis of the resuspended precipitate reveals the presence of fibrils (Figure 1 a)).

3.1.2 Protocol #2

DMSO is a highly polar, water-miscible organic solvent which is also commonly used to solubilize Aß peptides. In a vast majority of toxicity studies on cells, highly concentrated Aß (e.g. 5 mM) is dissolved in 100% DMSO and then diluted with PBS [42] or in cell culture medium [12]. Its effect on aggregation is very controversial. Some studies have demonstrated that Aß40 and Aß42 in pure DMSO remain stable in a monomeric α-helical structure and give rise to the so called “unaggregated Aß peptides preparations”, or “unaggregated fibril-free preparations” [12, 43], since DMSO prevents the organization of Aß in ß-sheet structures by hindering the formation of hydrogen bonds [12, 37, 44]. Other experiments instead clarified that 100% DMSO is not sufficient to maintain a monomeric solution [37]. Finally, other papers reported that when pure DMSO is diluted with buffer or water, it can immediately induce the formation of oligomeric aggregates and protofibrils [12, 37]. To shed light on these controversial data, in protocol #2 (Figure S1) either pure or phosphate buffer-diluted DMSO is used as redissolution solvent of the HFIP-dried film. As compared to protocol #1, protocol #2 is intended to obtain smaller oligomeric populations or even a single homogeneous monomeric population. The addition of 20% DMSO to Aß42 samples does not affect CE profiles and oligomerization, as compared to the results in Figure 1 a) (data not shown). By addition of either 50% or 100% of DMSO the aggregation process is comparable, thus in Figure 2 only results obtained with 100% DMSO as solubilizing solvent are reported. Peaks are labelled as in the electropherograms of Figure 1 a), because they are identified on the basis of statistically equal electrophoretic mobilities, therefore it is plausible to hypothesize that the size distribution is similar. Peaks A, B and C are detected together with other minor species.

Conversely to what claimed by Stine *et al.* in a seminal work [37], here the electropherogram at t0 clearly indicates that sample preparation using HFIP and then pure DMSO does not produce a single, uniform and unaggregated sample. The use of DMSO as solubilizing agent ensures a longer time window where

oligomers are kept soluble if compared to that obtained by following protocol #1; in particular, the first migrating population (peak A) is detected at very long times after redissolution. However, neither are fibrils present immediately after solubilization nor at the end of the process: Aß42 prepared according to protocol #2 precipitates as amorphous aggregates after about one month from t0. This could explain also the observed absence of dynamic equilibrium between oligomers (Figure S4). Another limitation that hinders any further investigation is that the CE data obtained feature a DMSO concentration that is not only toxic for neuroblastoma cells but also chemically incompatible with ultrafiltration devices.

3.1.3 Protocol #3

By preparing the sample according to protocol #1 multiple equilibria are observed by CE, i.e. that between faster (peak A) and slower (peaks B and C) migrating species and that between the putative bigger assemblies (peak B and peak C). However, the putative small oligomers rapidly contribute to the formation of large aggregates by progressively decreasing peak A area, so that little information about smaller species is obtained.

In order to shift the aggregation process further towards low molecular weight oligomers, Aß42 was solubilized following a protocol previously set up [29]. To accurately replicate what reported by Bartolini *et al.* the peptide here used was purchased by the same supplier (Bachem). After preparing the sample according to this protocol (here defined as protocol #3, Figure S1), Aß42 is injected in CE and its self-assembly is monitored over time by an optimized CE method (method B). This method considerably shortens analyses times (less than 7 min), in turn it allows more frequent sampling and improves efficiency. By a multimethodological approach, in [20] authors demonstrated and/or inferred the formation of assemblies ranging from monomers up to decamers immediately after solubilization, and of higher MW oligomers including protofibrils within the first 12-48 hours, before sample precipitation.

In Figure 3a) it is clear that at t0 the sample already includes at least three main electrophoretic peaks as well as amyloid fibrils, which are observed by TEM. That protocol #3 is less aggregating than the first protocol is also evident: soluble species are detected for longer times, including two earlier migrating and very narrow peaks. This could be explained by the longer contact of lyophilized Aß peptide with HFIP and by the treatment with a basic mixture in ACN, so to keep a non amyloidogenic conformation [29].

In Figure 3a), mobilities are calculated as average of 5 independent experiments using three peptide batches from the same supplier. Effective mobilities are statistically different from those reported in Figure 1a), except for those of the fastest migrating peak, where values fall within the experimental errors, equal to two times the standard deviation [45]. However, they are labelled as peak 1, 2 and 3.

Analogously to what shown by others [22] minor species are also visible and nevertheless they are not taken into consideration in this study, given the low abundance and the absence of dynamic equilibrium. From electrophoretic traces Figure 3a) and from the graph in Figure 3b) it emerges that the faster migrating population consists of two peaks at dynamic equilibrium: peak 1 slowly contributes to the formation of peak 2. As for protocol #1, the reproducibility of the normalized area percent is very good (SD < 8%). A progressive reduction of both peaks 1 and 2 area is observed, while a slower migrating broad band (peak 3) is built up. Therefore, as compared to protocol #1 (Figure 1), the aggregation is slowed down to such an extent that an equilibrium among the putative small species is appreciable by CE. Aß42 oligomers are soluble for about one month until precipitation into amyloid fibrils.

An issue that is rarely raised by authors who report studies on Aß42 is the very high variability of commercial peptides with regard to solubility and in turn aggregation properties. To our knowledge, a single systematic study on different Aß42 suppliers, however limited to the effect on fibril polymorfism, was reported [13].

In particular methods of synthesis and purification could be source of variability. Notably, batch-to-batch variations in the declared degree of purity may be found, as well as different instructions for standard peptide solubilization within the same supplier and among different suppliers. In our experience this problem can not be neglected and this is the reason why, to support their robustness, all CE data are here averaged on different batches purchased from the same supplier.

Notably, when Aß42 supplied by Anaspec is solubilized according to protocol #3, it shows the same electrophoretic profile of the Bachem peptide (data not shown). Conversely, when Aß42 provided by Bachem is solubilized by following protocol #1, precipitation occurs after 30 minutes from t0, when soluble species are not detected, the sample is visibly cloudy and TEM analysis shows fibrils (Figure S5). These data confirm the high variability of synthetic peptides and suggest that a given protocol cannot be applied to any purchased peptide standard but it strongly depends on the supplier. Therefore it is imperative to have a tool suitable to verify peptide solubility.

3.2 Aß42 oligomer characterization

3.2.1 CE analyses of ultrafiltrated samples

Highly reproducible CE analyses of soluble oligomers over a wide time window are the necessary premises for a reliable characterization of the separated species.

In order to assign a range of MW to the oligomers analytically separated by CE and prepared by protocols #1 and #3, ultrafiltration experiments are carried out with different cutoff membranes. Solutions to be ultrafiltrated have been selected at appropriate elapsed times from solubilization, depending on the

favourable relative abundance of the peak areas observed in CE. In principle ultrafiltration is not devoid of limitations, as it can only assign a molecular weight range and adsorption phenomena may affect sample recovery and data interpretation. Nevertheless this approach is very simple, fast, and CE analyses serve as a control of the oligomeric state, by comparison between unfiltered, retained and filtrated solutions. In general, it is reasonable to consider that, while the amount found in filtrated solutions has to be entirely ascribed to actual filtrated protein material, the amount found in the retained solution can partly be constituted by aggregated peptide adsorbed on the filter and not necessarily retained in virtue of its size. Oligomers ranging from trimers up to dodecamers migrate under peak A (protocol #1): peak A is totally retained on 10 kDa (Figure 4d)), mostly on 30 kDa (Figure 4 c)) and filtrated through 50 kDa membrane (Figure 4 b)). Based on these evidences, the bands corresponding to Aß42 dimers detected by SDS-PAGE/Western Blot (Figure S2) must definitely be ascribed to an artefact due to oligomer disaggregation induced by SDS: as seldom reported [14, 46], it can be concluded that SDS-PAGE, despite its widespread usage, does not mimic the actual conditions in solution. The slower migrating peaks B and C correspond to aggregates smaller than 22-mers and larger than dodecamers, since they are quantitatively recovered in the filtrated solution of 100 kDa cutoff and in the retained solution of 50 kDa cutoff (Figure 4 a) and b)), respectively.

Along with what stated for peaks B and C and based on membrane specifications, ultrafiltration on 50 and 100 kDa membranes (Figure 4 a) and b)) shows that peak 3 corresponds to aggregates larger than dodecamers and that no aggregates bigger than 100kDa (22-mers) are present in solution. Considering the low recovery of peak 3 in the filtrated solution, it is assumed that part of the peptide is entrapped in the filter. On the other hand, the size distribution of small assemblies is different from protocol #1. Identification of peaks 1 and 2 a from monomers up to hexamers is revealed by electropherograms of samples filtrated on 10 and 30 kDa membranes (Figure 4 d) and c)).

Membrane specifications for 30 kDa and 10 kDa devices make us reasonably hypothesize that peaks 1 and 2 correspond to monomers and dimers, respectively. By simple ultrafiltration experiments the presence of monomers and dimers in solution, as demonstrated in [20], is confirmed. It is valuable that in this work the presence of soluble Aß oligomers is monitored for much longer time

3.2.2 ATR-FTIR characterization of the secondary structure of Aß42 oligomers

The conformational features of the different Aß42 oligomers obtained by protocol #1 and protocol #3 were investigated by ATR-FTIR spectroscopy. This approach provides information on the peptide secondary structures and intermolecular interactions through the analysis of the Amide I band (around 1700-1600 cm^{-1}) manly due to the stretching vibration of the C=O peptide group [32, 33, 47]. Figure 5a) shows the FSD spectra of the peptide films of Aß42 solubilized by protocol #1 (at 2.5 h) before and after ultrafiltration through a 50 kDa cutoff membrane. The spectra of the whole peptide and of the retained assemblies are

characterized by an intense peak around 1630 cm^{-1} and by a minor component around 1695 cm^{-1}, both assigned to ß-sheet structures [31]. The intensity of the ~1630 cm^{-1} component decreases in the filtrated solution indicating a lower ß-sheet content in this sample (Figure 5a)). The intensity ratio 1695/1630, called ß-index, has been suggested to be proportional to the percentage of antiparallel ß-sheet in the structure and has been widely employed in the FTIR analyses of Aß and other amyloidogenic polypeptides [32]. The ß-index values calculated from the baseline corrected FSD spectra of Aß42 solubilized by protocol #1 (Figure 5b)) are within the range expected for Aß peptide oligomers with a predominantly antiparallel organization of the ß-sheets [31, 32, 48]. For a semi-quantitative comparison of the ß-sheet content in the different samples, a curve-fitting analysis on the FSD spectra was performed (Figure 5c) and Figure S6-FTIR1). The entire peptide preparation and the retained solution are characterized by a higher amount of ß-sheets (average ± SD: 62.74% ± 4.87 and 66.76% ± 1.68, respectively) as compared to that of the filtrated solution (48.60% ± 3.31). These findings are in agreement with the characterization obtained by ultrafiltration (Figure 4 b)) and mirror the differences in apparent molecular mass among oligomers filtrated and retained by 50 kDa cutoff membrane.

The same ATR-FTIR analyses were performed on the Aß42 peptide solubilized by protocol # 3, immediately after solubilization (Figure 5). This sample is characterized by the lowest amount of ß-sheet structures (Figure 5a) and 5c)) and by the highest ß-index value (Figure 5b)) as compared to the Aß42 peptides solubilized by protocol #1. We should note that the ~1695 cm^{-1} component is well resolved in the entire peptide and retained solution from protocol #1 while it is more overlapped with the near components in the filtrated solution from protocol #1 and in the entire peptide solution from protocol #3, leading to a possible overestimation of the ß-index value, markedly in the last case.

Since dehydration can affect the polypeptide secondary structures, particularly in the case of disordered proteins and peptides [49], we performed control experiments to compare the infrared response of Aß42 samples measured in form of a thin film (Figure 5 and Figure S6-) with that of Aß42 samples measured in solution (Figure S7). Very similar ATR-FTIR results were obtained with and without solvent evaporation for the entire peptide and retained solution from protocol #1. In the case of the filtrated sample from protocol #1 and of the entire peptide from protocol #3, the analyses of the ATR-FTIR spectra collected in solution indicate a lower content of ß-sheets and a higher α-helical/random coil structures (Figure S7), compared to secondary structures of the same Aß42 samples measured as a peptide film (Figure 5, Figure S6). In particular, the content of ß-sheet structures of the different Aß42 samples measured in solution was found to decrease in the following order (Figure S7-FTIR2): protocol #1, retained (65.10% ± 3.31); protocol #1, 2.5h (61.39% ± 4.53); protocol #1, filtrated (40.32% ± 8.03); protocol #3, t0 (26.96% ± 5.69). These data are consistent with ultrafiltration results (Figure 4d)). Altogether, the ATR-FTIR analyses of the different Aß42 samples measured as a thin peptide film or in solution consistently indicate a progressive increase of the ß-

sheet structures in the conversion of smaller species into larger assemblies, in agreement with what expected from their size.

3.3 Toxicity studies

The possibility to isolate aggregates by ultrafiltration also allows to consider these oligomeric populations as independent targets in toxicity tests, i.e. to verify whether aggregates of different size are endowed with different toxicity.

In vitro and *ex-vivo* toxicity of different Aß42 oligomers is controversial [9, 35, 36]; moreover, in this respect the supplier-to supplier variability of the synthetic Aß42 peptide is not addressed by the literature.

First, the ability of Aß42 *in toto* of inducing cell death on SH-SY5Y neuroblastoma cells was verified. For these experiments, cells were exposed to Aß42 (solubilized by following sample preparation protocol #3) after 10 days from solubilization, when both small and large oligomers are present. Compared to the control, 10 µM Aß42 induced a significant loss of cell viability (average ± SD : 79.44% ± 4.12, Figure 6). In the same fashion, toxicity experiments were independently carried out on oligomers filtrated and retained by a 50 kDa membrane (see Figure 4b) as explicative electrophoretic profiles). It is evident that monomers and dimers (peak 1 and 2) do not affect cell viability. Conversely, oligomers bigger than dodecamers (peak 3 in the electrophoretic pattern) are responsible for the toxicity of the entire Aß42 peptide, since they induce a cell death to an extent similar to that induced by the peptide *in toto* (cell viability, average ± SD : 80.09% ± 1.82).

4. CONCLUSIONS

Notwithstanding decades of research, the relationship between size, structure and toxicity of Aß42 oligomers remains unclear, also because of the difficulties in setting-up *in vitro* methods, to study the dynamic formation of such oligomers, to characterize the observed species and to independently assign toxicity. Since our pioneering work [21, 26-28], a few attempts have been made to describe Aß42 oligomerization *in vitro* by using CE as the main tool. CE separations published so far are almost exclusively confined to two main oligomeric populations that are rapidly precipitating and for which a dynamic equilibrium is often not demonstrated. These difficulties are unavoidably associated to poor peak area accuracy and reproducibility and make the applications of the methods intrinsically limited.

Here we have instead presented, over a wide time window, standardized and very reproducible analyses of soluble oligomeric populations that show multiple equilibria. When prepared by three different protocols, different aggregation dynamics of Aß42 peptide is clearly appreciated and accurately described. By a simple injection in CE we have also shown that a given sample preparation protocol may not be applicable to synthetic Aß42 peptides from different suppliers.

Conversely to what previously found by us, by ultrafiltration experiments followed by CE analyses monomers and dimers are detected using a less aggregating sample preparation (protocol #3), whereas by a more aggregating protocol (protocol #1), trimers represent the smallest specie formed. This finding is in contrast with what obtained by SDS-PAGE Western Blot, as it is highly possible that the formation of dimeric forms of Aß42 is an artefact of SDS-induced disaggregation [14, 46].

CE gives immediate access to semi-quantitative data on the proteinaceous material present in solution, on the dynamic formation of soluble oligomeric assemblies over time and on the reproducibility of the process. This means that CE preserves the native state of aggregates and should play a primary role in this kind of studies on aggregating peptides. The isolation of the separated species unequivocally identifies the absence of toxicity of oligomers with an apparent molecular mass lower than 50 kDa, namely equal or smaller than dodecamers, in particular monomers and dimers.

For the first time Aß42 oligomers isolated from a solution where they are at dynamic equilibrium are subjected to ATR-FTIR investigations through measurements both as a peptide film and in solution. Interestingly, the differences found in secondary structures are in agreement with the different oligomeric size distribution of the aggregates, as assessed by ultrafiltration. Indeed, α-helical/random coil structures are most abundant in smaller species, whereas a higher ß-sheet content characterizes the bigger and more toxic Aβ42 assemblies.

The integrative use of TEM, ATR-FTIR and cell-based assays clarifies and corroborates the results of the CE analysis. For all these reasons this approach is now adequate and complete enough to identify potential anti-oligomerization molecules and may help screening campaigns in drug discovery for Alzheimer's disease.

5. ACKNOWLEDGEMENTS

This work was supported by the University of Pavia (PhD student grant to FB); and by the University of Milano-Bicocca (research grant Fondo di Ateneo per la Ricerca to AN).

6. REFERENCES

[1] B. Winblad, P. Amouyel, S. Andrieu, C. Ballard, C. Brayne, H. Brodaty, A. Cedazo-Minguez, B. Dubois, D. Edvardsson, H. Feldman, L. Fratiglioni, G.B. Frisoni, S. Gauthier, J. Georges, C. Graff, K. Iqbal, F. Jessen, G. Johansson, L. Jonsson, M. Kivipelto, M. Knapp, F. Mangialasche, R. Melis, A. Nordberg, M.O. Rikkert, C. Qiu, T.P. Sakmar, P. Scheltens, L.S. Schneider, R. Sperling, L.O. Tjernberg, G. Waldemar, A. Wimo, H. Zetterberg, Defeating Alzheimer's disease and other dementias: a priority for European science and society, Lancet Neurol, 15 (2016) 455-532.

[2] S. Da Mesquita, A.C. Ferreira, J.C. Sousa, M. Correia-Neves, N. Sousa, F. Marques, Insights on the pathophysiology of Alzheimer's disease: The crosstalk between amyloid pathology, neuroinflammation and the peripheral immune system, Neurosci Biobehav Rev, 68 (2016) 547-562.

[3] S.J. Lee, E. Nam, H.J. Lee, M.G. Savelieff, M.H. Lim, Towards an understanding of amyloid-beta oligomers: characterization, toxicity mechanisms, and inhibitors, Chem Soc Rev, 46 (2017) 310-323.

[4] H.W. Querfurth, F.M. LaFerla, Alzheimer's disease, N Engl J Med, 362 (2010) 329-344.

[5] F. Chiti, C.M. Dobson, Protein Misfolding, Amyloid Formation, and Human Disease: A Summary of Progress Over the Last Decade, Annu Rev Biochem, 86 (2017) 35.1-35.42.

[6] A. Jan, O. Adolfsson, I. Allaman, A.L. Buccarello, P.J. Magistretti, A. Pfeifer, A. Muhs, H.A. Lashuel, Abeta42 neurotoxicity is mediated by ongoing nucleated polymerization process rather than by discrete Abeta42 species, J Biol Chem, 286 (2011) 8585-8596.

[7] J.A. Hardy, G.A. Higgins, Alzheimer's disease: the amyloid cascade hypothesis, Science, 256 (1992) 184-185.

[8] G. Bitan, M.D. Kirkitadze, A. Lomakin, S.S. Vollers, G.B. Benedek, D.B. Teplow, Amyloid beta -protein (Abeta) assembly: Abeta 40 and Abeta 42 oligomerize through distinct pathways, Proc Natl Acad Sci U S A, 100 (2003) 330-335.

[9] I. Benilova, E. Karran, B. De Strooper, The toxic Abeta oligomer and Alzheimer's disease: an emperor in need of clothes, Nat Neurosci, 15 (2012) 349-357.

[10] D.M. Walsh, D.J. Selkoe, A beta oligomers - a decade of discovery, J Neurochem, 101 (2007) 1172-1184.

[11] A. Jan, D.M. Hartley, H.A. Lashuel, Preparation and characterization of toxic Abeta aggregates for structural and functional studies in Alzheimer's disease research, Nat Protoc, 5 (2010) 1186-1209.

[12] W.B. Stine, L. Jungbauer, C. Yu, M.J. LaDu, Preparing synthetic Abeta in different aggregation states, Methods Mol Biol, 670 (2011) 13-32.

[13] M.Y. Suvorina, O.M. Selivanova, E.I. Grigorashvili, A.D. Nikulin, V.V. Marchenkov, A.K. Surin, O.V. Galzitskaya, Studies of Polymorphism of Amyloid-beta42 Peptide from Different Suppliers, J Alzheimers Dis, 47 (2015) 583-593.

[14] J.M. Mc Donald, G.M. Savva, C. Brayne, A.T. Welzel, G. Forster, G.M. Shankar, D.J. Selkoe, P.G. Ince, D.M. Walsh, The presence of sodium dodecyl sulphate-stable Abeta dimers is strongly associated with Alzheimer-type dementia, Brain, 133 (2010) 1328-1341.

[15] M.R. Nichols, B.A. Colvin, E.A. Hood, G.S. Paranjape, D.C. Osborn, S.E. Terrill-Usery, Biophysical comparison of soluble amyloid-beta(1-42) protofibrils, oligomers, and protofilaments, Biochemistry, 54 (2015) 2193-2204.

[16] D.C. Rambaldi, A. Zattoni, P. Reschiglian, R. Colombo, E. De Lorenzi, In vitro amyloid Abeta(1-42) peptide aggregation monitoring by asymmetrical flow field-flow fractionation with multi-angle light scattering detection, Anal Bioanal Chem, 394 (2009) 2145-2149.

[17] S.L. Bernstein, N.F. Dupuis, N.D. Lazo, T. Wyttenbach, M.M. Condron, G. Bitan, D.B. Teplow, J.E. Shea, B.T. Ruotolo, C.V. Robinson, M.T. Bowers, Amyloid-beta protein oligomerization and the importance of tetramers and dodecamers in the aetiology of Alzheimer's disease, Nat Chem, 1 (2009) 326-331.

[18] A. Abelein, J.D. Kaspersen, S.B. Nielsen, G.V. Jensen, G. Christiansen, J.S. Pedersen, J. Danielsson, D.E. Otzen, A. Graslund, Formation of dynamic soluble surfactant-induced amyloid beta peptide aggregation intermediates, J Biol Chem, 288 (2013) 23518-23528.

[19] S. Matsumura, K. Shinoda, M. Yamada, S. Yokojima, M. Inoue, T. Ohnishi, T. Shimada, K. Kikuchi, D. Masui, S. Hashimoto, M. Sato, A. Ito, M. Akioka, S. Takagi, Y. Nakamura, K. Nemoto, Y. Hasegawa, H. Takamoto, H. Inoue, S. Nakamura, Y. Nabeshima, D.B. Teplow, M. Kinjo, M. Hoshi, Two distinct amyloid beta-protein (Abeta) assembly pathways leading to oligomers and fibrils identified by combined fluorescence correlation spectroscopy, morphology, and toxicity analyses, J Biol Chem, 286 (2011) 11555-11562.

[20] M. Bartolini, M. Naldi, J. Fiori, F. Valle, F. Biscarini, D.V. Nicolau, V. Andrisano, Kinetic characterization of amyloid-beta 1-42 aggregation with a multimethodological approach, Anal Biochem, 414 (2011) 215-225.

[21] S. Sabella, M. Quaglia, C. Lanni, M. Racchi, S. Govoni, G. Caccialanza, A. Calligaro, V. Bellotti, E. De Lorenzi, Capillary electrophoresis studies on the aggregation process of beta-amyloid 1-42 and 1-40 peptides, Electrophoresis, 25 (2004) 3186-3194.

[22] D. Brinet, J. Kaffy, F. Oukacine, S. Glumm, S. Ongeri, M. Taverna, An improved capillary electrophoresis method for in vitro monitoring of the challenging early steps of Abeta1-42 peptide oligomerization: application to anti-Alzheimer's drug discovery, Electrophoresis, 35 (2014) 3302-3309.

[23] D. Brinet, F. Gaie-Levrel, V. Delatour, J. Kaffy, S. Ongeri, M. Taverna, In vitro monitoring of amyloid beta-peptide oligomerization by Electrospray differential mobility analysis: An alternative tool to evaluate Alzheimer's disease drug candidates, Talanta, 165 (2017) 84-91.

[24] R. Picou, J.P. Moses, A.D. Wellman, I. Kheterpal, S.D. Gilman, Analysis of monomeric Abeta (1-40) peptide by capillary electrophoresis, Analyst, 135 (2010) 1631-1635.

[25] R.A. Picou, I. Kheterpal, A.D. Wellman, M. Minnamreddy, G. Ku, S.D. Gilman, Analysis of Abeta (1-40) and Abeta (1-42) monomer and fibrils by capillary electrophoresis, J Chromatogr B Analyt Technol Biomed Life Sci, 879 (2011) 627-632.

[26] R. Colombo, A. Carotti, M. Catto, M. Racchi, C. Lanni, L. Verga, G. Caccialanza, E. De Lorenzi, CE can identify small molecules that selectively target soluble oligomers of amyloid beta protein and display antifibrillogenic activity, Electrophoresis, 30 (2009) 1418-1429.

[27] S. Butini, M. Brindisi, S. Brogi, S. Maramai, E. Guarino, A. Panico, A. Saxena, V. Chauhan, R. Colombo, L. Verga, E. De Lorenzi, M. Bartolini, V. Andrisano, E. Novellino, G. Campiani, S. Gemma, Multifunctional cholinesterase and amyloid Beta fibrillization modulators. Synthesis and biological investigation, ACS Med Chem Lett, 4 (2013) 1178-1182.

[28] S. Brogi, S. Butini, S. Maramai, R. Colombo, L. Verga, C. Lanni, E. De Lorenzi, S. Lamponi, M. Andreassi, M. Bartolini, V. Andrisano, E. Novellino, G. Campiani, M. Brindisi, S. Gemma, Disease-modifying anti-Alzheimer's drugs: inhibitors of human cholinesterases interfering with beta-amyloid aggregation, CNS Neurosci Ther, 20 (2014) 624-632.

[29] M. Bartolini, C. Bertucci, M.L. Bolognesi, A. Cavalli, C. Melchiorre, V. Andrisano, Insight into the kinetic of amyloid beta (1-42) peptide self-aggregation: elucidation of inhibitors' mechanism of action, Chembiochem, 8 (2007) 2152-2161.

[30] M.T. Ackermans, F.M. Everaerts, J.L. Beckers, Quantitative analysis in capillary zone electrophoresis with conductivity an indirect UV detection, J Chrom A, 549 (1991) 345-355.

[31] E. Cerf, R. Sarroukh, S. Tamamizu-Kato, L. Breydo, S. Derclaye, Y.F. Dufrene, V. Narayanaswami, E. Goormaghtigh, J.M. Ruysschaert, V. Raussens, Antiparallel beta-sheet: a signature structure of the oligomeric amyloid beta-peptide, Biochem J, 421 (2009) 415-423.

[32] R. Sarroukh, E. Goormaghtigh, J.M. Ruysschaert, V. Raussens, ATR-FTIR: a "rejuvenated" tool to investigate amyloid proteins, Biochim Biophys Acta, 1828 (2013) 2328-2338.

[33] A. Natalello, S.M. Doglia, Insoluble protein assemblies characterized by fourier transform infrared spectroscopy, Methods Mol Biol, 1258 (2015) 347-369.

[34] A. Natalello, P.P. Mangione, S. Giorgetti, R. Porcari, L. Marchese, I. Zorzoli, A. Relini, D. Ami, G. Faravelli, M. Valli, M. Stoppini, S.M. Doglia, V. Bellotti, S. Raimondi, Co-fibrillogenesis of Wild-type and D76N beta2-Microglobulin: the crucial role of fibrillar seeds, J Biol Chem, 291 (2016) 9678-9689.

[35] G.M. Shankar, S. Li, T.H. Mehta, A. Garcia-Munoz, N.E. Shepardson, I. Smith, F.M. Brett, M.A. Farrell, M.J. Rowan, C.A. Lemere, C.M. Regan, D.M. Walsh, B.L. Sabatini, D.J. Selkoe, Amyloid-beta protein dimers isolated directly from Alzheimer's brains impair synaptic plasticity and memory, Nat Med, 14 (2008) 837-842.

[36] S. Lesne, M.T. Koh, L. Kotilinek, R. Kayed, C.G. Glabe, A. Yang, M. Gallagher, K.H. Ashe, A specific amyloid-beta protein assembly in the brain impairs memory, Nature, 440 (2006) 352-357.

[37] W.B. Stine, Jr., K.N. Dahlgren, G.A. Krafft, M.J. LaDu, In vitro characterization of conditions for amyloid-beta peptide oligomerization and fibrillogenesis, J Biol Chem 278 (2003) 11612-11622.

[38] D. Thirumalai, G. Reddy, J.E. Straub, Role of water in protein aggregation and amyloid polymorphism, Acc Chem Res, 45 (2012) 83-92.

[39] K. Klement, K. Wieligmann, J. Meinhardt, P. Hortschansky, W. Richter, M. Fandrich, Effect of different salt ions on the propensity of aggregation and on the structure of Alzheimer's abeta(1-40) amyloid fibrils, J Mol Biol, England, 373 (2007) 1321-1333.

[40] M. Garvey, K. Tepper, C. Haupt, U. Knupfer, K. Klement, J. Meinhardt, U. Horn, J. Balbach, M. Fandrich, Phosphate and HEPES buffers potently affect the fibrillation and oligomerization mechanism of Alzheimer's Abeta peptide, Biochem Biophys Res Commun, 409 (2011) 385-388.

[41] M. Kato, H. Kinoshita, M. Enokita, Y. Hori, T. Hashimoto, T. Iwatsubo, T. Toyo'oka, Analytical method for beta-amyloid fibrils using CE-laser induced fluorescence and its application to screening for inhibitors of beta-amyloid protein aggregation, Anal Chem, 79 (2007) 4887-4891.

[42] F. Yin, J. Liu, X. Ji, Y. Wang, J. Zidichouski, J. Zhang, Silibinin: a novel inhibitor of Abeta aggregation, Neurochem Int, 58 (2011) 399-403.

[43] C.L. Shen, R.M. Murphy, Solvent effects on self-assembly of beta-amyloid peptide, Biophys J, 69 (1995) 640-651.

[44] K. Broersen, W. Jonckheere, J. Rozenski, A. Vandersteen, K. Pauwels, A. Pastore, F. Rousseau, J. Schymkowitz, A standardized and biocompatible preparation of aggregate-free amyloid beta peptide for biophysical and biological studies of Alzheimer's disease, Protein Eng Des Sel, 24 (2011) 743-750.

[45] M. Quaglia, E. De Lorenzi, Capillary electrophoresis in drug discovery, Methods Mol Biol, 572 (2009) 189-202.

[46] A.D. Watt, K.A. Perez, A. Rembach, N.A. Sherrat, L.W. Hung, T. Johanssen, C.A. McLean, W.M. Kok, C.A. Hutton, M. Fodero-Tavoletti, C.L. Masters, V.L. Villemagne, K.J. Barnham, Oligomers, fact or artefact? SDS-PAGE induces dimerization of beta-amyloid in human brain samples, Acta Neuropathol, 125 (2013) 549-564.

[47] A. Barth, Infrared spectroscopy of proteins, Biochim Biophys Acta, 1767 (2007) 1073-1101.

[48] M. Baldassarre, C.M. Baronio, L.A. Morozova-Roche, A. Barth, Amyloid β-peptides 1-40 and 1-42 form oligomers with mixed β-sheets, Chem Sci, 8 (2017) 8247-8254).

[49] A. Natalello, V.V. Prokorov, F. Tagliavini, M. Morbin, G. Forloni, M. Beeg, C. Manzoni, L. Colombo, M. Gobbi, M. Salmona, S.M. Doglia, Conformational plasticity of the Gerstmann-Straussler-Scheinker disease peptide as indicated by its multiple aggregation pathways, J Mol Biol, 381 (2008) 1349-1361.

FIGURE LEGENDS

Figure 1. Protocol #1. Oligomerization process of Aß42 monitored over time by CE (method A). a) Top: representative electrophoretic profiles of Aß42 (221 µM) at different elapsed times from t0 until sample precipitation and average effective electrophoretic mobilities (μ_{eff}) of detected peaks, (n=5 independent experiments). Insets: representative TEM images of amyloid fibrils at t0 and at sample precipitation, (n=3); scale bar: 100 nm. Bottom: average, SD and relative standard deviation (RSD) of μ_{eff} of detected peaks. **b)** Plot of the normalized peak area % at different elapsed times of peak A, peak B and peak C, during the first 30 hours, when dynamic equilibrium is evident. Each monitoring point is in triplicate, error bars correspond to SD.

Figure 2. Protocol #2. Oligomerization process of Aß42 monitored over time by CE (method A, redissolution in 100% DMSO). Monitoring of Aß42 (221 µM) aggregation process from t0 up to 28 days, CE traces are representative of n=3 independent experiments. The off-scale EOF signal is truncated for clarity. Inset: representative TEM image of amorphous aggregates observed at t0 and at sample precipitation; scale bar: 100 nm.

Figure 3. Protocol #3. Oligomerization process of Aß42 monitored over time by CE (method B). a) Top: representative electrophoretic profiles of Aß42 (100 µM) at different elapsed times from t0 until the end of aggregation process, (n=5 independent experiments). Inset: amyloid fibrils identified by TEM analysis at t0 and at sample precipitation; scale bar: 100 nm. Bottom: average, SD and RSD of μ_{eff} of detected peaks. b) Plot of the normalized peak area % over time of peak 1, peak 2 and peak 3. Each monitoring point is in triplicate, error bars correspond to SD.

Figure 4. UF characterization of Aß42 oligomers. Ultrafiltration experiments with a) 100, b) 50, c) 30 and d) 10 kDa with Aß42 solubilized by following protocol #1 and protocol #3.

Figure 5. ATR-FTIR characterization of Aß42 oligomers. a) FSD spectra of different Aß42 preparations showed in the Amide I band. b) The ß-index values (intensity ratio ~1695/~1630) calculated from the baseline corrected FSD spectra. c) Total content of the ß-sheet structures evaluated by curve-fitting analysis of the FSD spectra. The ATR-FTIR spectra were collected after solvent evaporation, corrected for the buffer absorption and normalized at the Amide I band area before FSD. The reported data refer to the average and standard deviation obtained from three independent Aß42 preparations. Analysed samples: Aß42 from protocol # 1 before ultrafiltration (Prot #1, 2.5h), retained (Prot #1 R, 2.5 h) and filtrated (Prot #1 F, 2.5 h) through a 50 kDa membrane; entire Aß42 peptide solubilized by protocol # 3 (Prot #3 t0).

Figure 6. MTT test. Entire Aß42 peptide and oligomers lower and bigger than 50 kDa (sample preparation protocol #3, 10 days). Data are expressed as cell viability of control, error bars represent SD (n=3).

Figure

Click here to download high resolution image

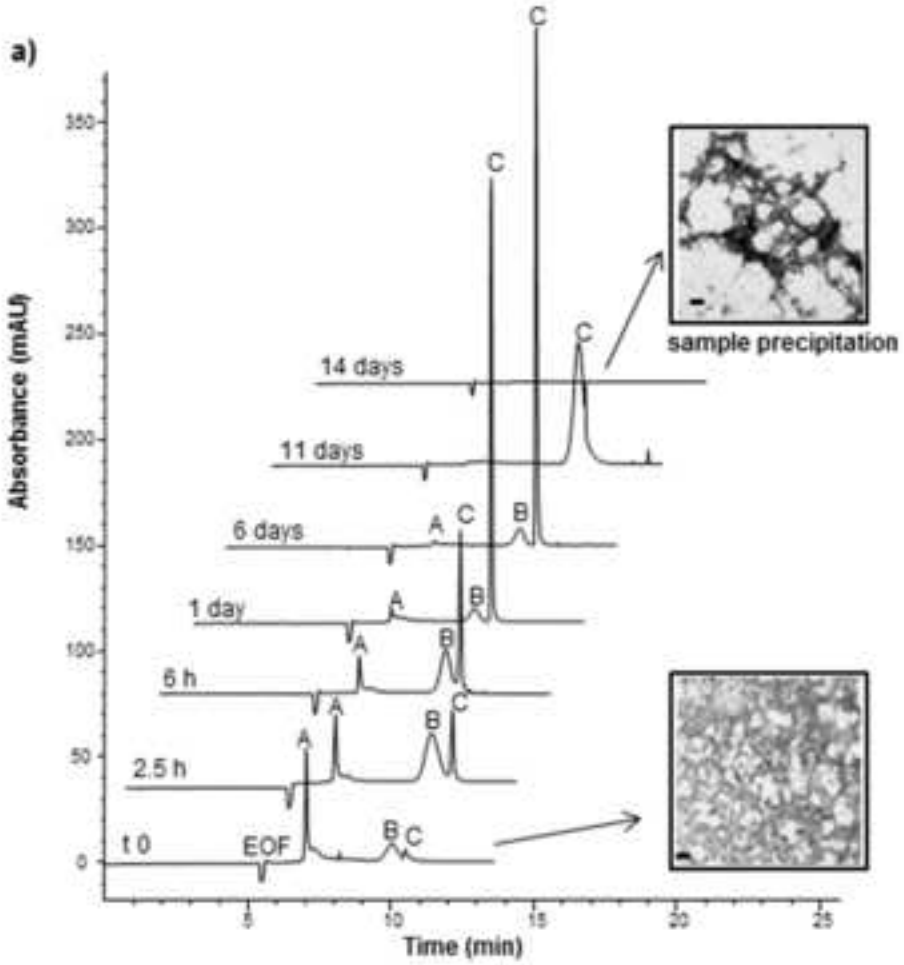

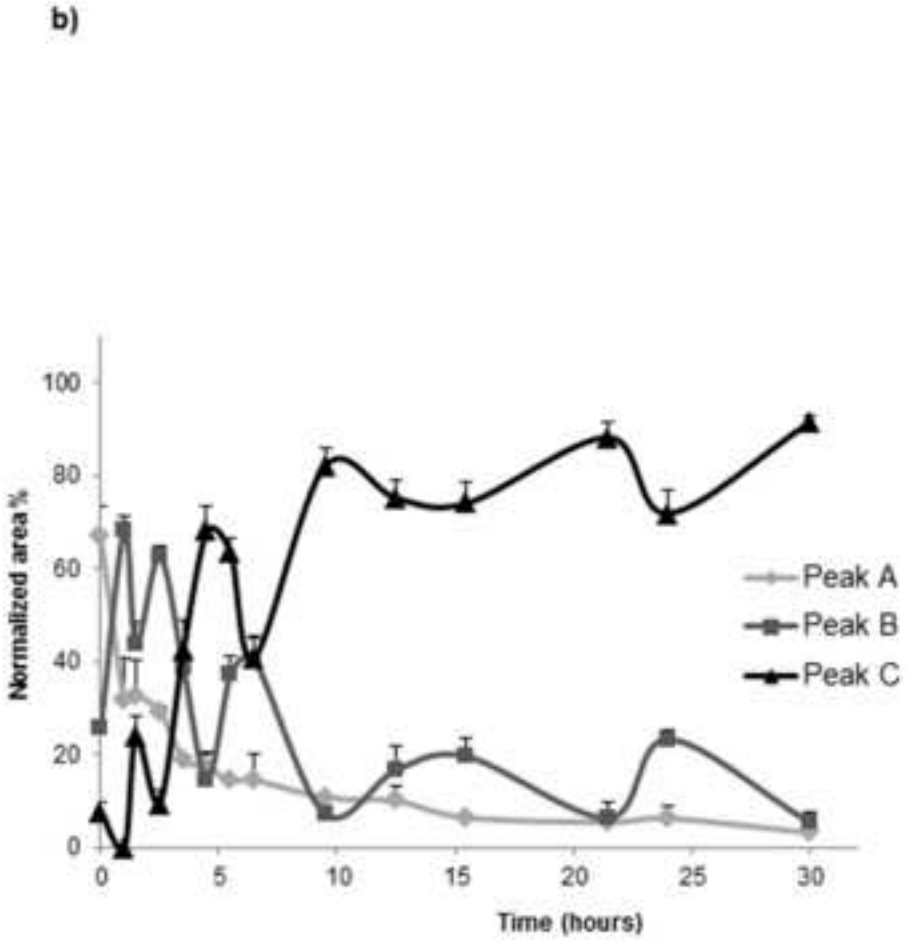

	Peak A	Peak B	Peak C
Average μ_{eff} ($cm^2V^{-1}s^{-1}$)	-9.93×10^{-5}	-2.01×10^{-4}	-2.17×10^{-4}
SD (n=50)	$\pm 5.73 \times 10^{-7}$	$\pm 1.75 \times 10^{-6}$	$\pm 2.17 \times 10^{-6}$
RSD	0.57%	0.87%	0.99%

Figure

Click here to download high resolution image

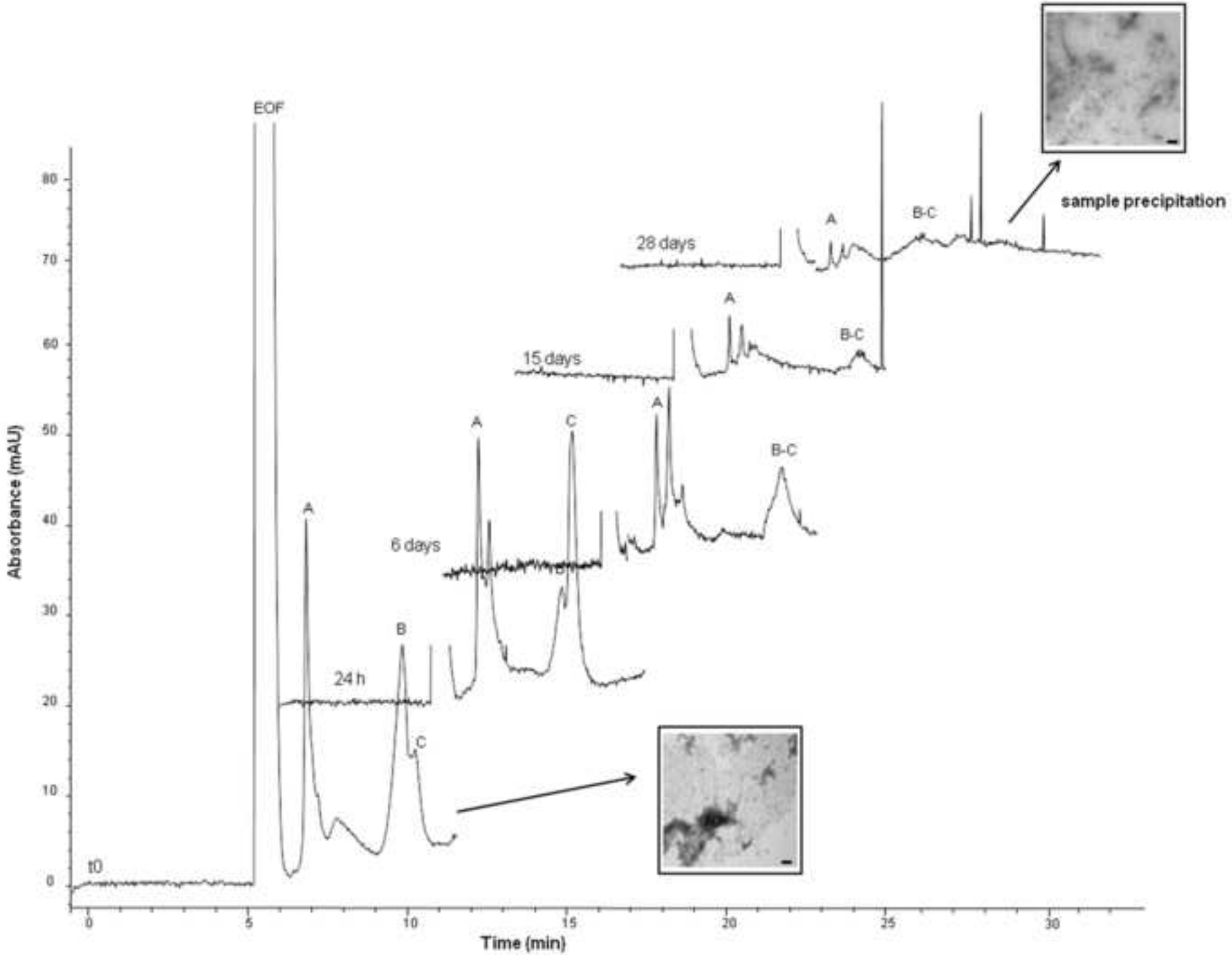

Figure

Click here to download high resolution image

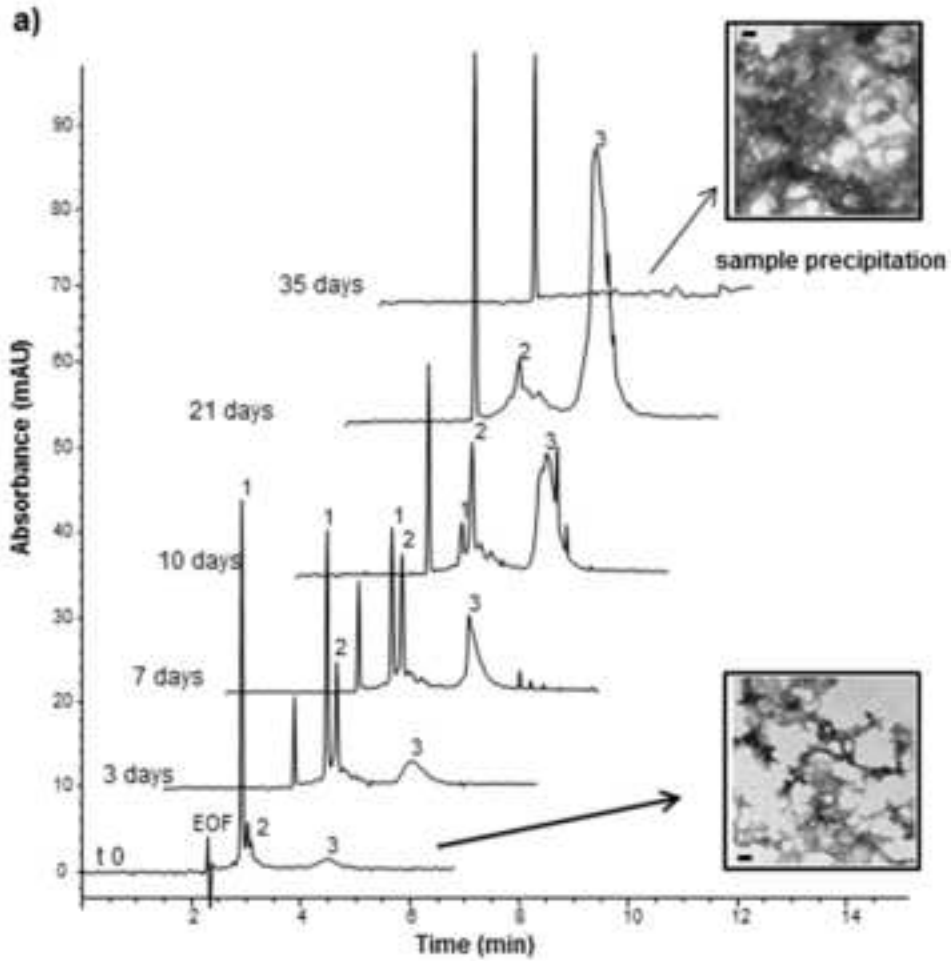

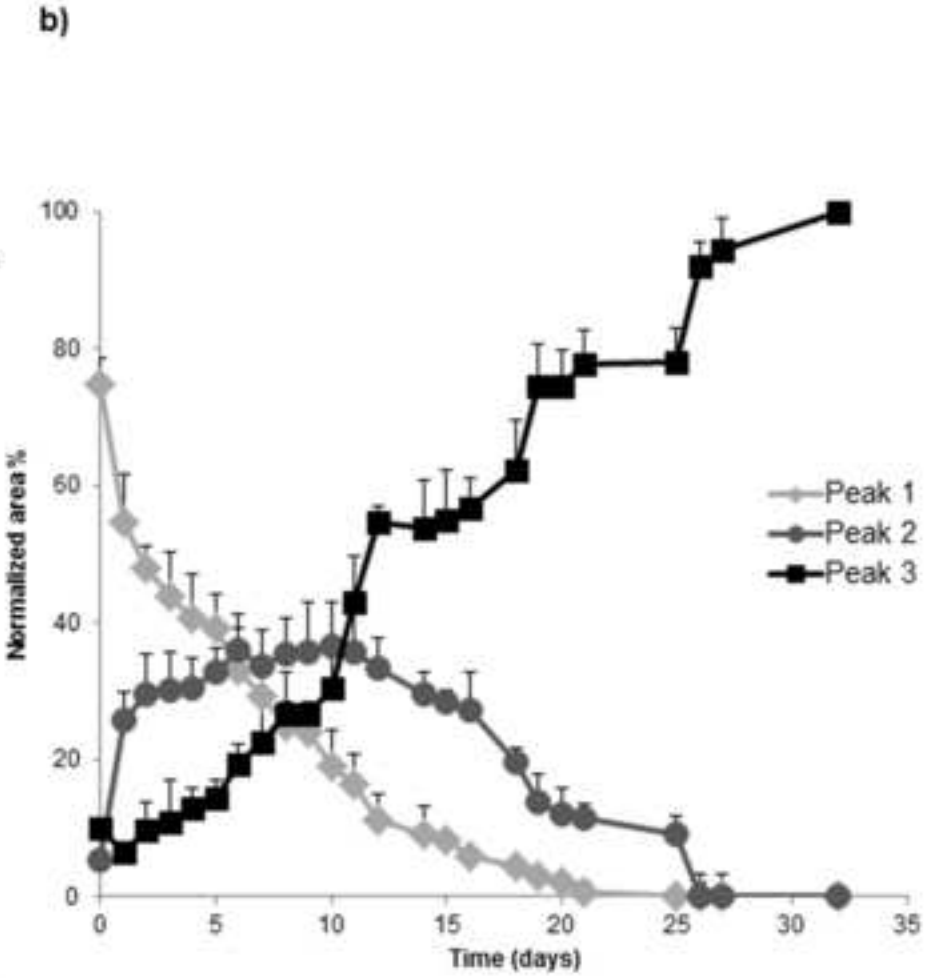

	Peak 1	Peak 2	Peak 3
Average μ_{eff} ($cm^2V^{-1}s^{-1}$)	-9.79×10^{-5}	-1.19×10^{-4}	-2.36×10^{-4}
SD (n=50)	$\pm 5.78 \times 10^{-7}$	$\pm 1.13 \times 10^{-6}$	$\pm 2.18 \times 10^{-6}$
RSD	0.59%	0.95%	0.92%

Figure

Click here to download high resolution image

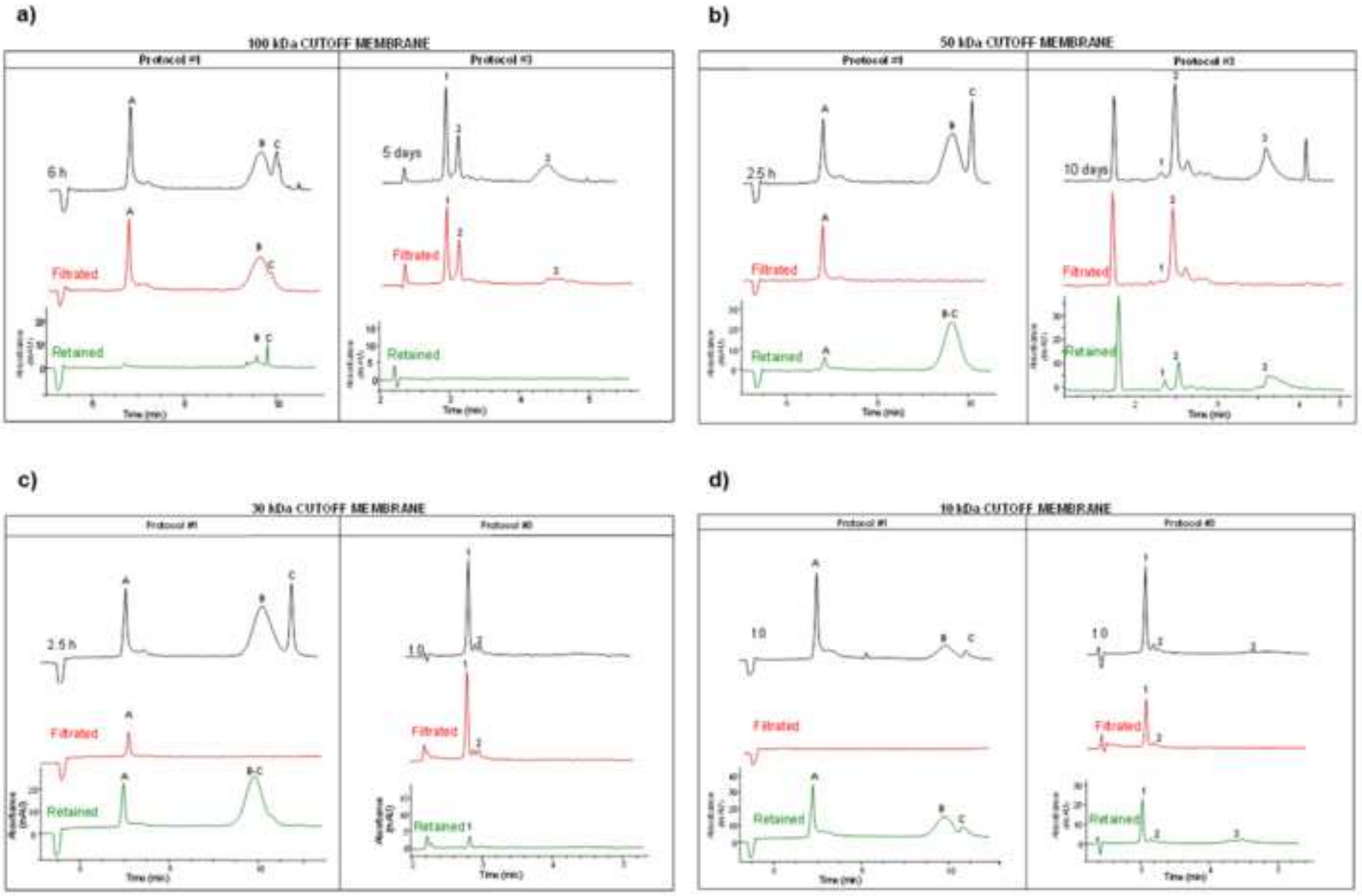

Figure

Click here to download high resolution image

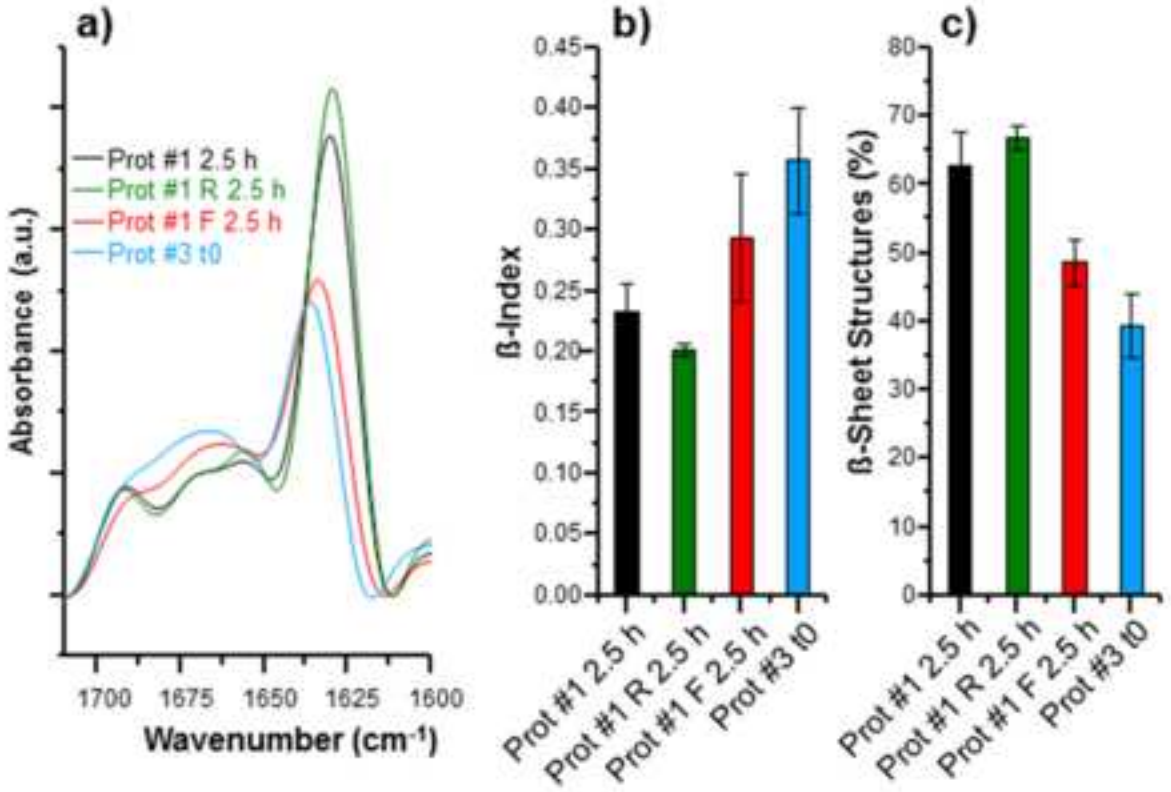

Figure

Click here to download high resolution image

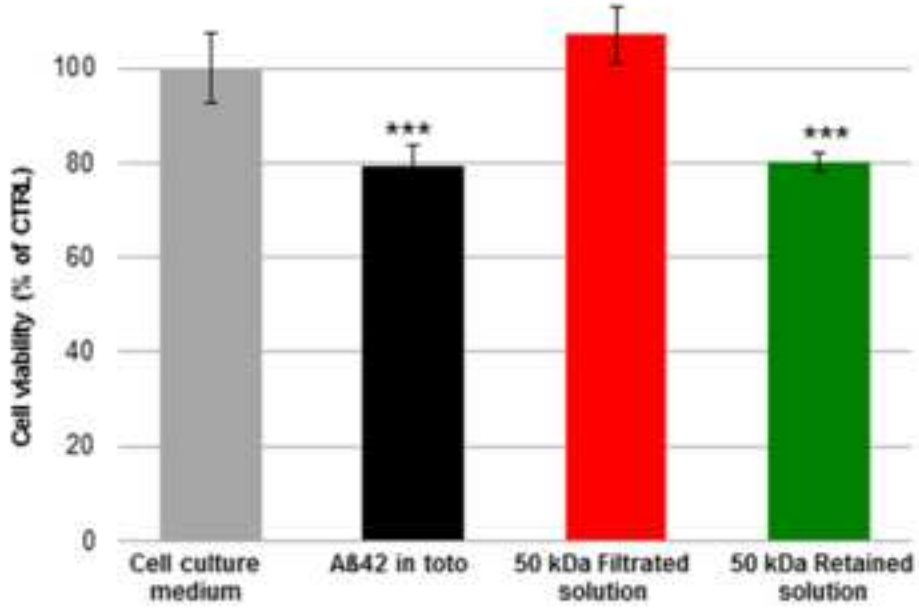

Checklist

- Cover letter
- Novelty statment
- Highlights
- Manuscript
- Figures
- List of potential reviewers
- Supplementary
- Graphical abstract

***List of Three Potential Reviewers**

1. Andreas Barth
   Department of Biochemistry and Biophysics, Stockholm University, Arrhenius Laboratories, Svante Arrhenius väg 16, 106 91 Stockholm, Sweden
   Expert in protein analysis by ATR-FTIR

   andreas.barth@dbb.su.se

2. Manuela Bartolini
   Department of Pharmacy and Biotechnology, University of Bologna, Via Belmeloro 6, 40126 Bologna, Italy
   Expert in analysis of Abeta and of Abeta aggregation

   manuela.bartolini3@unibo.it

3. Hanno Stutz
   Division of Chemistry and Bioanalytics, University Salzburg, Hellbrunnerstrasse 34, 5020 Salzburg, Austria
   Expert in protein analysis by Capillary electrophoresis

   hanno.stutz@sbg.ac.at

Supplementary Material

Click here to download Supplementary Material: Supplementary Material.docx

*Graphical Abstract (for review)

Click here to download high resolution image